UNIVERSITY OF OKLAHOMA

GRADUATE COLLEGE

RHEOLOGY OF AQUEOUS AND POLYMER-BASED NITROGEN FOAMS AT HIGH PRESSURE AND HIGH TEMPERATURE (HPHT) CONDITIONS

A THESIS

SUBMITTED TO THE GRADUATE FACULTY

in partial fulfillment of the requirements for the

Degree of

MASTER OF SCIENCE IN NATURAL GAS ENGINEERING AND MANAGEMENT

By

TAREK FIROZE AKHTAR
Norman, Oklahoma
2017

RHEOLOGY OF AQUEOUS AND POLYMER-BASED NITROGEN FOAMS AT HIGH PRESSURE AND HIGH TEMPERATURE (HPHT) CONDITIONS

A THESIS APPROVED FOR THE
MEWBOURNE SCHOOL OF PETROLEUM AND GEOLOGICAL ENGINEERING

BY

_____
Dr. Ramadan Ahmed, Chair

_____
Dr. Subhash Shah

_____
Dr. Saeed Salehi

This thesis is dedicated to my family, friends and everyone else, who have made me realize that one must not strive for success, but excellence instead.

Acknowledgements

Firstly, I am grateful to be blessed with God's blessings as He has time and again, with the guidance of Islam, given me the strength and determination to achieve all goals I have set my mind to at any given point of life, provided I be patient.

Next, I would like to thank Dr. Ramadan Ahmed for his continued support and patience as an advisor and supervisor during my tenure at OU as a graduate student. His immense knowledge of fluid dynamics has gotten out the best of me and has helped in truly delivering my full potential as a research student. Last but not the least, his patience is truly admirable as it teaches one a lot of life lessons.

I would also like to specifically thank my fellow students: Rida El Gaddafi, Soham Pandya, Testi Sherif and Vimlesh Bavadiya, who have taken time out to help me during my times of need to troubleshoot several issues throughout the course of this research.

Additionally, I would like to thank Dr. Subhash Shah and Dr. Saeed Salehi for taking time out to be part of my committee. I have truly enjoyed the experience of being under their guidance as a graduate student.

Furthermore, none of the experiments would have been possible, had it not been for the diligent efforts of the equipment specialist, Jeff McCaskill. Besides being a friend, colleague, and fellow Pink Floyd fan, his experience and wisdom has truly been a pillar of support throughout my time as a researcher at the Well Construction Technology Center.

This research was made possible by NPRP grant 5-059-2-020 from the Qatar National Research Fund (QNRF). I would like to express my gratitude and appreciation

to the QNRF for sponsoring the research and University of Oklahoma for the use of equipment and facilities at the Well Construction Technology Center.

Lastly, I would like to thank my parents who have constantly supported me in all my academic endeavors for past twenty odd years. They have always guided me during the toughest of times and this thesis would not be possible without their support.

Table of Contents

List of Tables

List of Figures

Abstract

Foams are complex mixtures of gas and liquid held together by a surfactant at the gas-water interface. The use of foams find application in many industrial operations such as underbalanced drilling fluid, fracturing fluid in well stimulation, injection fluid in enhanced oil recovery technique, and fire-extinguishing agent in firefighting. Applicability of foam depends on its viscosity and stability. Rheological behavior of foams is mainly a function of foam quality (i.e. gas volume fraction), base liquid viscosity, pressure and temperature. The method of foam generation and foam stability are also factors that affect its rheology. Foams are of two main types when used for underbalanced drilling purposes: aqueous foams and polymer-based foams.

This thesis presents results of experimental investigation conducted to study the effects of foam quality, pressure and wall slip on aqueous and polymer-based foam rheology. It also seeks to establish a new method for the prediction of yield stresses. Flow experiments were performed using a foam recirculating flow loop that has three pipe viscometers in parallel configuration. Experiments on aqueous foams were carried out at ambient temperature (23.8 ± 1% °C), and varying pressures (6.89 13.79 and 20.68 MPa). Tests on polymer-based foams were conducted at high pressure (6.89 MPa) and varying temperatures (23.2, 76.7 and 107.2 °C). All tests were performed using three pipe viscometers with different diameters (3.06, 6.22 and 12.67 mm). Pressure losses across the viscometers were measured at different flow rates (0.1 to 1.1 L/min). Foam was generated by flowing a mixture of base liquid (water/water +0.25% PAC with 2% surfactant) and nitrogen through a needle valve. Pressure drop across the valve was measured and maintained approximately at a constant value (298.8 kPa). Before each

measurement, foam was regenerated by circulating the fluid at the maximum flow rate. All measurements were taken in laminar flow. Results indicate strong non-Newtonian behavior of foam, which closely fits the power law model for shear rate range considered in this investigation. Noticeable flow curve shifting, which may be an indication of wall slip, was not observed when tests were conducted varying pipe size. Secondary pressure effect, which is foam viscosity change because of pressure variation at a constant foam quality, was negligible but rheology variations at high temperatures were seen for polymer-based foams. High quality foams (quality greater than 65%) displayed yielding behavior when the flow is gradually reduced to zero.

Chapter 1: Introduction

1.1 Overview

Foams are colloidal dispersions made up of gas in liquid along with a surfactant. They have drawn interest for quite a while because of their widespread occurrence in everyday life. Some of these examples include whipped cream as a food product, commercial bottle cleaning process foam as a detergent, shaving foam as a personal care product, and sewage treatment of effluent foams in process industries amongst others. Foams have characteristic properties that may be desirable such as in the case of fire-fighting foams or undesirable as foaming in gas-oil separators (Schramm 1994). Foams being highly viscous and light fluids, earlier found applications in the oilfield have been for reservoir injection (Claude et al. 1968) and hydraulic fracturing (Khalil and de Franco 1989). Presently, it is also used as a drilling fluid for underbalanced drilling.

Conventional drilling utilizes the concept of overbalance using drilling fluids such as water-based muds wherein the wellbore pressure is maintained above the formation pressure. This is done to prevent a kick, which is unintentional influx of any formation fluid during drilling. The well must be shut-in if a kick is encountered. Loss of well control can result in a disastrous blowout of the well. Underbalanced drilling is a method of drilling wherein the wellbore pressure is held lower than the formation pressure to intentionally allow the influx of formation fluids while drilling (Gas Research Institute 1997). Low-density drilling fluids such as air, foams and natural gas are used to achieve the desired underbalance pressure. Produced formation fluids are

diverted to a separator while allowing the drill string to continue rotation by utilizing a rotating head at the surface.

Underbalanced drilling is typically used in low-pressure formations and has several benefits such as increased penetration rates, low risks associated with differential sticking and lost circulation, reduced formation damage with little or no stimulation requirements and production of lucrative formation fluids while drilling resulting in a quicker payout.

In foam drilling, foam is generated at the surface by mixing the compressed gas stream with a foaming solution from the liquid injection pump (Fig. 1.1). Nitrogen and air are often used as the gaseous phase. Due to its bubble structure, foam provides a lifting capacity superior to that of any drilling fluid. Foam quality is adjusted by controlling back-pressure, and gas and liquid injection rates. The control allows the operator to produce the desired underbalanced wellbore pressure, which also maintains well stability.

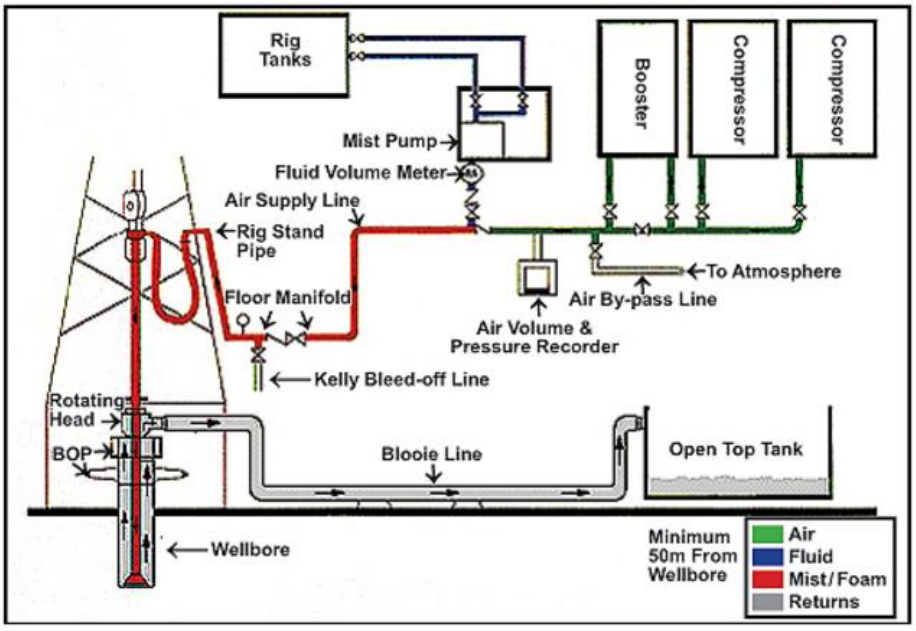

Figure 1.1 Schematic of underbalanced drilling using mist/foam (Source: Viking Drilling 2017)

The drawbacks of foam drilling include requirements of additional equipment such as compressive, booster, separator and nitrogen unit. Moreover, it is required to generate foam and maintain underbalanced conditions at all times while drilling. Furthermore, high associated costs of surfactant and defoamer needed to break down foam are some other limitations.

Foams are thermodynamically unstable, and a system that uses it must be meticulously monitored to prevent instability issues. Foam structure at a given state is primarily attributed to the size of the bubbles and how they are arranged with respect to each other. While at static flow conditions, foams experience gravity drainage of the liquid phase along with the coalescing of foam bubbles, causing the liquid phase to segregate as time passes. Thus, studying it under dynamic flow conditions is important to prevent such issues. Nonetheless, predicting foam behavior is never an easy task as

dynamic foam flow implies variations in viscosity, density and flow rate as the temperature, pressure, and shear rate changes.

The use of foam as drilling fluid in the hydraulic program requires a thorough review of rheological parameters for evaluating and determining the bottom hole pressure and surface injection-rate requirements. The rheological properties of foams are quite different from its constituent liquid and gas. They depend on foam quality, operating temperature and pressure, base liquid properties, foam generation method.

Poly Anionic Cellulose (PAC) is a biopolymer commonly used as a viscosifier and a filtration control additive in water-based drilling fluids. Physically, it is a white powder with a specific gravity ranging from 1.5 – 1.6. It also resists to bacterial attack, thus, requiring no biocides or preservatives when used. It's environmental acceptability and functionality over a wide range of salinity, hardness and pH levels make it an excellent additive. PAC in this study was used to generate polymer-based foams.

1.2 Problem Statement

Foam-based underbalanced drilling is especially suitable for drilling large holes in formations that are prone to lost circulation, low-pressure formations such as partially depleted reservoirs and in re-entry wells. As mentioned previously, this results in higher cuttings carrying capacity, increased penetration rates, low formation damage, reduced bit wear, eliminates differential sticking, reduces the risk of lost circulation and maximizes hydrocarbon recovery by requiring almost no clean up after drilling. Foam drilling annular velocities are quite low relative to other methods, and thereby, minimizes borehole erosion. It is also notable that high-quality foams used in the industry use a minimal amount of liquid.

While flowing in the annulus, downhole conditions continuously change and this, in turn, affects the foam properties. Thus, studying and understanding foam rheology at high pressures and temperatures at such dynamic conditions is imperative in terms of safety, reliability, and economics. This research, thus, investigates the effect of high pressures and high temperatures rheology of aqueous and polymer-based nitrogen foams using pipe viscometers.

1.3 Objective

The primary objective is to study the effect of high temperature and high pressure on the rheology of nitrogen foams. Nitrogen foams used in this study are of two kinds: aqueous foams with no additives and polymer-based foams with a PAC additive. Specific objectives include:

- Understanding foam behavior at high pressures and high temperatures upon evaluating foam rheology at the conditions using a pipe viscometer for a given foam generation method.
- Studying the effect of quality, pressure, and temperature on foam rheology.
- Developing correlations between foam quality and the rheological properties of foams.
- Evaluating presence of yielding and wall slip phenomena in pipe viscometers.

1.4 Methodology

The study objectives are accomplished using an experimental methodology. Upon reviewing relevant literature in foam rheology, a flow loop rated for high temperature and high pressure, to be used as a pipe viscometer setup was built using stainless steel tubing and valves to obtain accurate inline flow measurements. The loop consists of three 84 cm (33 1/8th in.) long pipe sections with inner diameters of 3.06 mm, 6.22 mm and 12.67 mm. (0.121 in., 0.245 in. and 0.495 in.). Three pipes with different diameters were chosen to detect wall slippage effect if present.

Relevant sensors such as differential pressure meters, a Coriolis flowmeter and pressure gauges were installed and the pipe viscometer measurements were validated with a standard rotational viscometer data using water and mineral oil. Identical

rheological results then ensured the validity of the pipe viscometer measurements. The setup has its own foam generation section and it is designed to measure foam rheology under equilibrium condition.

Aqueous and polymer-based nitrogen foams were investigated experimentally. PAC polymer was chosen due to its thermal stability, which is 148.9 °C (300°F) and the lack of requirement of a biocide to complement its use. Extensive experiments were conducted to collect high-quality data. The data is then analyzed to obtain the rheological flow behavior of the fluid being studied and investigate the presence of wall slip. Pressure drop measurements at static conditions after dynamic flow tests were also taken to determine the yielding behavior of the fluid. Furthermore, correlations were made using nonlinear regression techniques. These correlations related the physical parameters of the fluid to its flow behavior.

Chapter 2: Literature Review

Heller and Kuntamukkula (1987) lists several factors which might influence the flow behavior of foams, and should thus, be important in foam flow experiments: the ratio of mean bubble size to flow channel size; size distribution of bubbles; anisotropic bubble distribution during flow; wall interactions; flow geometry and flow rate; quality of foam being studied; properties of the two fluid phases; absolute pressure as it can be of significance due to the varying compressibility of the gases; concentration and type of the surfactant; interfacial rheological properties of foam and their variation with time. In this section, key points are covered in foam literature from a drilling perspective, namely: bubble structure, foam generation, rheology, stability, wall slippage and associated yield stresses.

2.1 Types of Drilling Foams Used in Existing Literature

Drilling foams are categorized based on both, the liquid phase and gaseous phase. From a liquid phase perspective, they are classified as stable foams and stiff foams. Stable foams are aqueous foams in which water along with surfactants and other additives such as corrosion inhibitors and salts constitutes the liquid phase. These additives do not influence the viscosity of the liquid phase (Gas Research Institute 1997). Numerous studies (Beyer et al. 1972; Bonilla and Shah 2000; Cawiezel and Niles 1987; Harris and Heath 1996; Herzhaft 1999; Kraynik 1988; Ozbayoglu et al. 2005; Patton et al. 1983; Sanghani and Ikoku 1983; and Thondavadi and Lemlich 1985) on aqueous foam have been carried out for several decades.

Stiff foams consist of an already viscosified liquid phase with additives such as hydroxypropyl guar (Enzendorfer et al. 1994; Harris 1985 1989; Phillips et al 1987; Tan

and McGowen 1991), xanthan gels (Sani et al. 2001), hydroxyethyl cellulose (Chen et al. 2007; Sherif et al. 2015), poly-anionic cellulose (Saintpere et al. 1999 and Babatola 2014) along with a surfactant. In addition, several studies (Bonilla and Shah 2000; Cawiezel and Niles 1987; Harris 1989; Harris and Heath 1996; Harris and Pippin 2000; Harris and Reidenbach 1987; Hutchins and Miller 2005; Khade and Shah 2004; Khan et al. 1988; Reidenbach et al. 1986; Rojas et al. 2001; Saintpere et al. 2000; Tan and McGowen 1991) were conducted on the stiff foams. The addition of viscosifier results in more viscous and stable foams as compared to those produced from a surfactant alone (Gas Research Institute 1997). Hence, it is common to refer stiff foams as gelled foams or polymer-based foams.

Recently, oil-based foams are introduced to drill water sensitive formations (Sherif et al. 2015; Sepulveda et al. 2008). Diesel or a blend of diesel and mineral oil along with an appropriate oil-soluble surfactant constitutes the liquid phase in these foams.

The most commonly used gas phases in oilfield foams are: air (Ball 2001; Blackwell and Sobolik 1987; Kraynik et al. 1986; Beyer et al. 1972; Chen et al. 2007; Gas Research Institute 1997; Ozbayoglu et al. 2005; Rojas et al. 2001; Saintpere et al. 2000; Sanghani and Ikoku ,1983), carbon dioxide (Kenyon 1993; Hutchins and Miller 2005; Phillips et al. 1987; Li et al. 2017; Reidenbach et al. 1986; Tan and McGowen 1991), nitrogen (Bonilla and Shah 2000; Cawiezel and Niles 1987; Enzendorfer et al. 1994; Harris 1985,1989; Harris and Heath 1996; Harris and Pippin 2000; Harris and Reidenbach 1987; Hutchins and Miller 2005; Khade and Shah 2004; Khan et al. 1988,

Patton et al. 1983; Sani et al. 2001; Thondavadi and Lemlich 1985; Wendorff and Earl 1983) and a mixture of nitrogen and carbon dioxide (Harris 1995).

2.2 Measurement of Foam Rheology

Hutchins and Miller (2005) state that it is imperative to utilize a pressurized apparatus for proper foam evaluation and discusses three types of viscometers used by researchers for evaluating foam rheology (Fig. 2.1). A Couette and Plane type viscometer, a type of rotational viscometer which assumes narrow slot approximation to replicate flow between parallel plates (Khan et al.,1988; Kroezen et al 1988; Princen 1984; Saintpere et al. 2000), a recirculating pipe viscometer (Bonilla and Shah 2000; Harris 1989; Harris and Heath 1996; Harris and Reidenbach 1987; Khade and Shah 2004; Reidenbach et al. 1986; Sani et al. 2001; Sherif et al. 2015) and a single pass viscometer (Cawiezel and Niles, 1987; Chen et al. 2005; Enzendorfer et al. 1994; Li et al 2017; Lourenço et al. 2003; Ozbayoglu et al. 2002 2005; Sanghani and Ikoku 1983; Wendorff and Earl 1983) are the major types of viscometers used for foam research purposes.

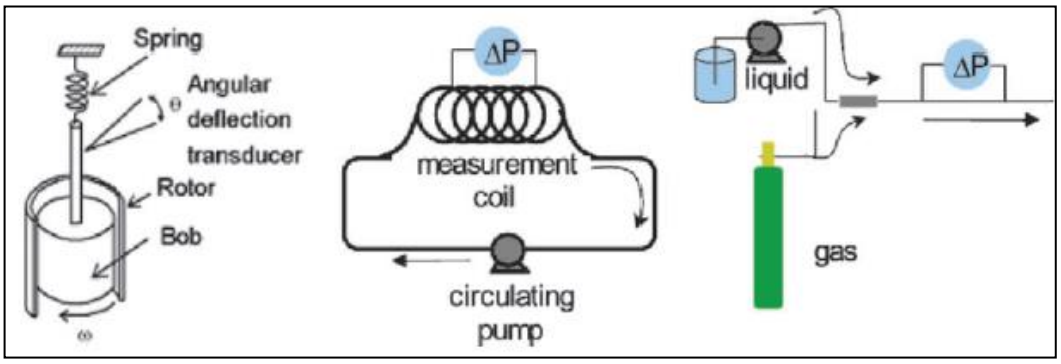

Figure 2.1 Rotational, recirculating and single pass viscometers (Hutchins and Miller 2005)

In rotational viscometer systems, the foam is first generated using an appropriate agitation method before taking rheological measurements (Khan et al. 1988; Kroezen et al. 1988). In recirculating and single-pass viscometers inline measurements are taken while the foam flowing. The foam is generated as it passes through a porous media, static mixers or special valves where foaming of the mixture occurs due to a pressure drop. Then, steady state pressure drop measurements are taken as the foam flows in the viscometer section. Recirculating viscometers are advantageous as the foam is equilibrated before recording pressure drop measurements and is also useful evaluating the time dependence of foam rheology. Hutchins and Miller (2005) presented a tabular summary (Fig. 2.2) of viscometers for foam rheology measurements stating their advantages, disadvantages, and suitability.

	Couette	Circulating Pipe	Single-Pass Pipe
Advantages	Time-dependent foam-property measurement Small sample size	Time-dependent foam-property measurement Easy foam visualization	Steady-state properties Easy foam visualization Easiest foam-generation method
Disadvantages	Foam containment Bubbles cream to top of cell Foam visualization is difficult	Foam structure may change as a result of the circulation system	Large sample size No time-dependent properties can be determined
Suitable for these conditions	Low pressure High-quality foam Stable foams	High pressure Any foam quality	High pressure Any foam quality

Figure 2.2 Summary of viscometers for foam rheology (Hutchins and Miller 2005)

2.3 Foam Generation

The method of foam generation before testing varies across existing literature and is possibly one of the reasons for conflicting results relating to foam studies

especially foam rheology. In some cases, foam is generated separately before measurement. Kroezen et al. (1988) uses a rotor-stator mixer to generate foams. In the rotor-stator mixers, gas and liquid containing surfactants are mixed by strong agitation, imparting kinetic energy. These mixers have a small mixing volume and continuously mix with large mixing intensity.

In pipe viscometers, foams are also produced using static mixers, porous media, or special valves by keeping them in-line to the flow. In a rotor-stator mixer, the energy is supplied by a rotating impeller to generate the foam whereas in a valve-type foam generator the dissipated energy is determined by the pressure drop, which arises in the mixing stream due to the gas-liquid flow. The foam generation can be controlled with the help of an appropriate valve opening and measurements of pressure drop across the flow as in the case of this study. The amount of energy supplied in the static mixer and foam structure obtained depend on the foam production rate and impeller speed and power. Rotor-stator mixers can be utilized over a greater production range and is advantageous in systems with a high liquid viscosity (Kroezen et al. 1988).

Khan et al. (1988) utilizes a foam generator, which makes foam by mixing a stream of gas and liquid solution containing surfactant in a porous structure such a steel wool mesh. Harris and Reidenbach (1987) utilized a recirculating flow-loop viscometer with stainless-steel tubing. The aqueous phase of the fluid was fed from a pressure vessel to the loop by a pump. The loop was filled with liquid to a pressure of 1,000 psi [6.9 MPa] by regulating the backpressure. N_2 addition would then generate foam by as the fluid flows through a small orifice into the loop while recirculating. By monitoring the change in specific gravity of the foam, excess fluid would be allowed to escape

through the backpressure regulator. Once the desired specific gravity was reached, the addition of N_2 was stopped and the fluid would be circulated for an additional period to equilibrate and develop foam structure. Bonilla and Shah (2000) utilized a similar methodology for recirculating pipe viscometers to generate foams. The liquid phase would first be drained gradually following which nitrogen gas is introduced into the recirculation loop to generate foam using a static mixer and gear pump at a pressure of 6.89 MPa (1000 psia)

2.4 Foam Rheology Models

The rheology of foams has been a subject of many experimental studies primarily due to common and conflicting findings. Amongst widely accepted conclusions are that, the rheology of foams depends on foam quality and the shear rate being applied to them, surfactant concentration has minor effect when varied among concentrations typically used for foams (Ahmed et al. 2003), and that the foam viscosity increases as a function of increasing base liquid viscosity (Mitchell 1971).

Mitchell measured foam rheology using small diameter tubes and relate foam viscosity, η_{foam} to the base liquid viscosity (η_L) and foam quality (Γ) as:

$$\eta_{foam} = \eta_L(1 + 3.6\Gamma);\ \Gamma \leq 54\% \tag{2.1}$$

$$\eta_{foam} = \eta_L(1 - \Gamma^{0.49})^{-1};\ \ \Gamma \geq 55\% \tag{2.2}$$

Foam flows are also characterized by bubble rupture and deformation. Rupturing affects the rheological properties of foams. For a steady homogenous shear flow at given shear rates, small changes in bubble shape from sphericity depends upon the capillary number Ca, which is expressed as:

$$Ca = \frac{a\gamma\eta_f}{\sigma} \tag{2.3}$$

where a, σ, γ and η_f denote average bubble radius, interfacial tension (surface tension), shear rate and foam viscosity, respectively (Ahmed et al. 2003).

As mentioned earlier in Section 2.2, Khan et al. (1988) used a parallel plate rotational viscometer to measure foam rheology and inferred that the Bingham plastic model best describes foam flow behavior. Beyer et al. (1972) measured the pressure drop of foam flow across 30.48 m (100 ft.) long pipes with varying diameter which act as a single pass viscometer. (13.87 18.85 and 24.31 mm, i.e., 0.546, 0.742 and 0.957 in.) Their results too fit foam rheology to the Bingham Plastic model, which is expressed as:

$$\tau - \tau_y = \frac{-\mu_o \varphi}{144} \tag{2.4}$$

where τ is the shear stress, τ_y is the yield stress, μ_o is the plastic bingham viscosity and φ is the shear rate.

Sanghani and Ikoku (1983) conducted foam rheology experiments using a concentric single pass annular viscometer and concluded that it is a power law fluid and demonstrated that flow behavior index and foam consistency index are functions of foam quality. In their study, an aqueous solution of foaming agent and air were simultaneously passed through the top of the drill pipe. The bottom of the drill pipe was perforated with four 2.38 mm (3/32 in.) holes, which act as nozzles and provide the necessary pressure drop for foaming. They proposed the following model to predict the apparent viscosity, μ_a of foam.

$$\mu_a = K\left(\frac{3n+1}{4n}\right)^n \left(\frac{8V}{D}\right)^{n-1} \tag{2.5}$$

In addition to Sanghani and Ikoku (1983), several studies (Enzendorfer et al. 1995; Hutchins and Miller 2005; Khade and Shah 2003; Kroezen et al. 1988; Patton et al. 1983; Sherif et. al 2005; Thondavadi and Lemlich 1988) reported power-law behavior of foam rheology.

Another experimental study (Cawiezel and Niles 1987) conducted at downhole conditions suggests that the Herschel-Bulkley model accurately describes foam rheology. An inconvenient drawback was that the empirical parameters be determined exactly for different foam systems encountered in a drilling operation.

Harris and Heath (1998) tested aqueous and polymer-based nitrogen foams at 6.89 MPa (1000 psia) for the use in fracturing using a recirculating pipe viscometer. They inferred that foam rheology obeys the Herschel-Bulkley model. Other studies (Reidenbach et al. 1986, Harris and Reidenback 1987, Harris 1995) on polymer-based foam conducted using recirculating pipe viscometers also concludes that foam rheology is best described by the Herschel-Bulkley model. The model developed by Reidenbach et al. (1986) expresses the apparent viscosity of foam as:

$$\mu_a = \left(\frac{4}{3}\right)^n \frac{\tau_y}{\frac{8V}{d}} + K_f \left(\frac{3n+1}{4n}\right)^n \left(\frac{8V}{D}\right)^{n-1} \tag{2.6}$$

Bonilla and Shah (2000) generated aqueous and gelled foams in their studies using a recirculating viscometer of two pipe sections of 12.7 and 9.5 mm (0.5 in. and 0.375 in.) at a pressure of 6.89 MPa (1000 psia) using varying temperatures of 23.9 – 79.4 °C (75– 175 °F). These foams too obeyed the Herschel-Bulkley model. Sani et al

(2001) also states the validity of the Herschel-Bulkley model with respect to foam rheology.

It was also seen in another study (Ozbayoglu et al. 2002) that foam rheology is more applicable to the Power Law model for 70% and 80% qualities, and the Bingham plastic model gives a better fit for 90% quality. Several rheological investigations on foam have recorded similar, yet sometimes conflicting results, thus, confirming that the method of foam generation and of how it is maintained while taking measurements is an important parameter to be considered while characterizing foams (Saintpere et al. 1999).

2.5 Foam Stability

Surfactants contain surface-active molecules known as micelles, which are responsible for the tendency of liquids to foam and the stability of the resulting bubbles. Surfactants have both hydrophilic and hydrophobic regions. At micelle concentrations higher than the Critical Micelle Concentration (CMC), spherical micelles organize themselves such that the hydrophobic ends protrude into the vapor and the hydrophilic heads are exposed to the liquid. This results in reduced surface tension for the respective foam fluid elements and gives stability to the foam structure. That is why pure liquid cannot foam without a surfactant. (Durian and Weitz 1994)

Rojas et al (2001) showed that the foam stability is a function of the surfactant concentration as it is increased up to 0.5% (by vol). Above this concentration, the foam stability remains constant, and the extra addition of a surfactant is not necessary due to the formation of spherical micelles as mentioned in the prior paragraph , close to a concentration called (CMC). Above this concentration, the interfacial free energy per

unit area, or surface tension of the bubbles formed is constant and consequently, the foam properties remain constant as well.

Time dependence of foam is one of the main reasons of the non-equilibrium nature of foams. As time varies, gravity drainage, coalescence of neighboring bubbles due to the rupture of the film boundary, and gas diffusion from smaller to bigger bubbles due to pressure difference is observed. These can be referred to as the aging mechanisms seen in foam (Durian and Weitz 1994).

Bubble coalescence in foams is not instantaneous and is prevented by other mechanisms involving surfactants, namely the Gibbs Elasticity and the Marangoni flow effects. The Gibbs effect occurs because thin film containing surfactant molecules tends to get stretched. The resultant increase in the film's surface area then tends to attract surfactant molecules to the surface causing surface tension to simultaneously increase. An equilibrium is established when proportions of the surfactant molecules at the surface and in the bulk of the fluid are no longer changing. At this point, there are fewer surfactant molecules per unit area of the surface. The Gibbs effect states that the stretched film will tend to contract elastically and hence referred to as the Gibbs elasticity effect.

The Marangoni flows effect arises due to a certain amount of time that surfactant molecules require to diffuse to the surface of a newly stretched film. Initially, the surface has very low concentration of surfactants, and the resultant surface tension is even greater than the calculated magnitude of Gibbs effect that one might predict. The surface tension gradually decreases to the Gibbs value as surfactants diffuse to the surface and the film equilibrates. Acting together, the Gibbs effect and

the Marangoni effect tend to stabilize infinitesimal fluctuations in foams (Kraynik et al. 1986). This is illustrated in Figs. 2.3 and 2.4.

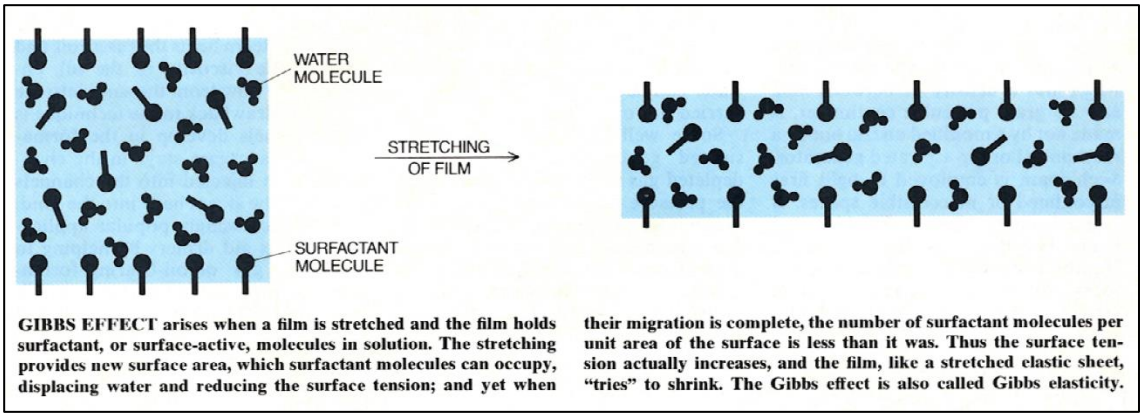

Figure 2.3 Illustration of Gibbs effect (Kraynik et al 1986)

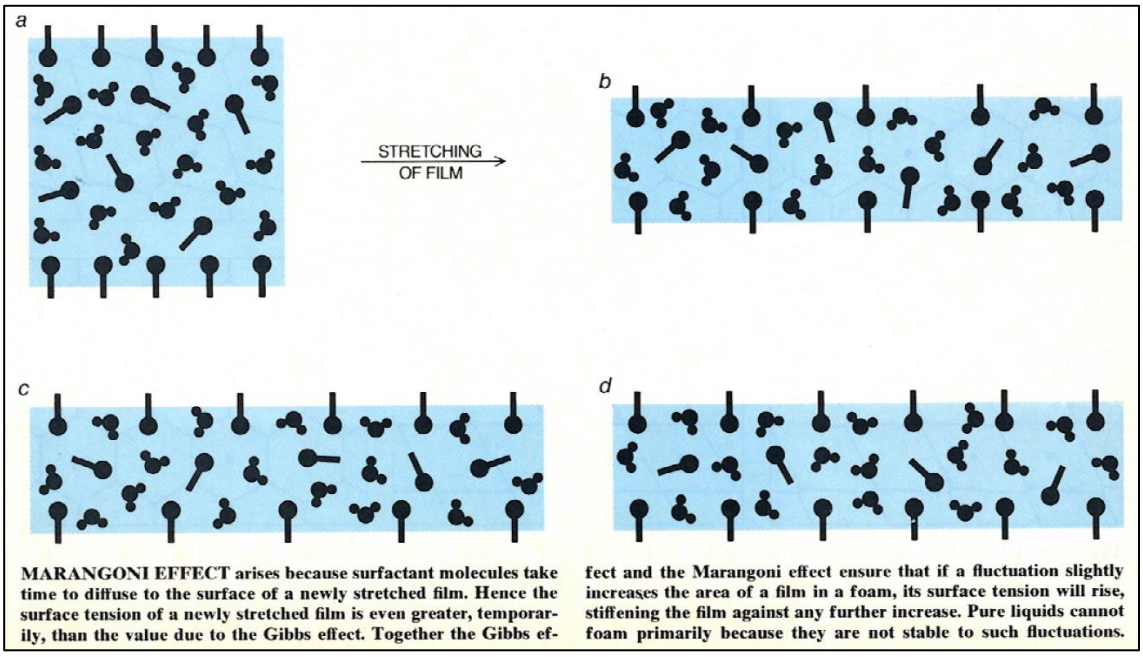

Figure 2.4 Illustration of Marangoni effect (Kraynik et al. 1986)

At experimental time scales, foams are stable and can be seen to have properties of all forms of matter. It can be solid like when it elastically responds to shearing due to the presence of a yield stress and fluid like due to its ability to flow and its compressible nature. In this study, a surfactant concentration of 2% was used to stay well above the CMC to have adequate surfactant for stable foam generation.

2.6 Foam Quality and Bubble Structure

Hutchins and Miller (2005) classified foams by quality, stating that they are dispersions, if foam quality is less than 52%; wet foams, if foam quality is between 52% and 74%; dry or polyhedral foam, if foam quality is between 74% and 96 %; and mist, if foam quality is less 96%. This is illustrated in Fig. 2.5.

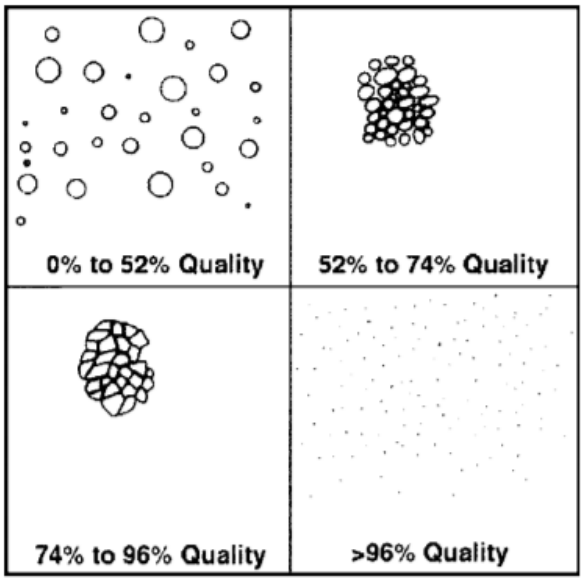

Figure 2.5 Bubble structure of foams at varying qualities (Hutchins and Miller 2005)

In a similar research, Ahmed et al. (2003) also stated how foam quality influences the structure of foam. Foam is said to be a "bubbly liquid" up to a given quality after which a rigidity transition takes place leading to the formation of well-structured spherical bubbles. For aqueous foams, the rigidity transition takes place at 63% (Holt and McDaniel 2000). Upon further increasing the quality, polyhedral bubbles with thin film borders are formed.

Foam viscosity is influenced primarily by foam quality and base liquid properties. The compressibility of the gas phase causes the quality to change when there is a change in pressure and temperature. Despite conflicting results in foam rheology experiments, it as a generally accepted notion that the foam viscosity increases

with quality (Ahmed et al 2003; Beyer et al 1972; Harris 1989; Mitchell 1971; Sanghani and Ikoku 1983; Sani et al 2001). The structural changes at different foam qualities are explicitly linked to the foam quality (Fig. 2.6).

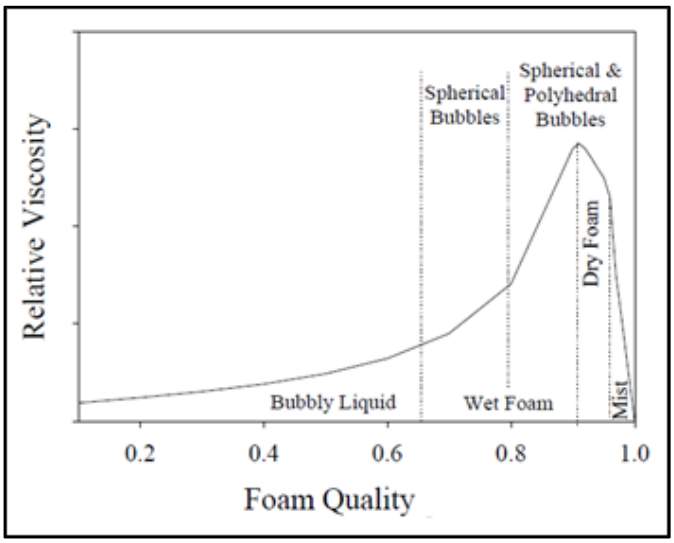

Figure 2.6 Relative Viscosity as a function of foam quality (Ahmed et al. 2003)

The primary distinction among foams is between wet and dry foams. In wet foam, the liquid content is high, and so the walls of the bubbles are thick. Hence, the bubbles tend to be spherical. Surface tension causes the bubbles to take a spherical shape by minimized surface area. As foam quality increases, its structure becomes more complex. The bubbles separate by thinner walls, and begin to influence one another. Thus, the spherical bubbles become polyhedral bubbles.

Kraynik et al (1986) mention that J. A. F. Plateau studied the structure of dry foams a century ago and states that the individual films forming the walls of the polyhedral bubbles in dry foams are supposed to be smooth surfaces with each having a uniform curvature. A curved film signifies a pressure difference between two adjacent bubbles. The pressure is greater inside the bubble (i.e. on the concave side of the

curve). It is also stated that the liquid in a polyhedral foam is distributed between films and Plateau borders, which are described as the channels that are formed at the point where films meet. The curvature of these borders indicates that the pressure inside a Plateau border is lower than the pressure in the bubbles and in the film. The resulting non-equilibrium state destabilizes and draws liquid out of the films. Although, at equilibrium states, which depend on foam stability, the surface force balance is such that most of the liquid in foam is in Plateau borders. When three films produce a Plateau border, the angles between them are equal, at 120 degrees, owing to a balance of surface-tension forces.

Foams are unstable fluids and undergo structural changes with time. The distribution of bubble size in foam is also subject to continuous change, primarily due to gas diffusion from bubbles with a large internal pressure to those with a smaller internal pressure. This causes small bubbles to become smaller, and large bubbles to grow larger. The bubble size distribution further changes when bubbles start to coalesce.

Durian and Weitz (1994) give an appropriate illustration (Fig. 2.7) showing the structure of foams and state that dry foams (i.e. foams with high gas content) tend to have polyhedral bubble structure with thin films of uniform thickness whereas wet foams (i.e. foams with high liquid content) have spherical bubbles. Dry foams and wet foams tend to exist together when foam structure starts to destabilize. Dry foams are lighter than wet foams and hence, are present in the top portions of degrading foam (Fig. 2.7).

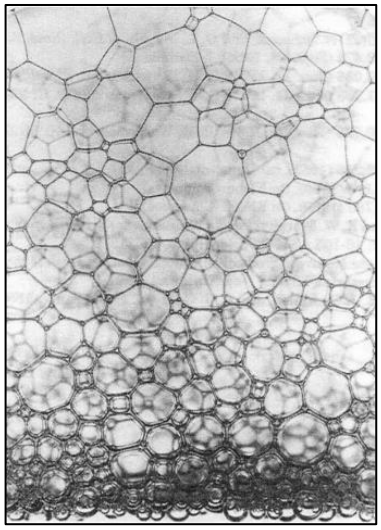

Figure 2.7 Dry foams at the top with polyhedral bubbles and wet foams at the bottom with spherical bubbles (Durian and Wietz 1994)

2.7 Effect of Pressure

It is known that at given conditions for a given foam quality, significant pressure increase implicitly reduces the existing foam quality and viscosity, and an increase in temperature at constant pressure conditions brings down the viscosity of the liquid phase, thus, affecting the foam viscosity (Beyer et al. 1972).

Gases in foam have varying compressibility at different pressures and thus, pressure is associated with the compressibility of foam, which directly related to its quality. Cawiezel and Niles (1987) while studying aqueous and gelled foam rheology utilized single pass viscometers and was conducted at high temperatures up to 79.4°C (175°F) and at high pressures up to 34.47 MPa (5000 psia) to mimic downhole conditions. Their research showed that increase in pressure resulted in a significant increase in foam viscosity for lower shear rates as compared to higher shear rates.

2.8 Effect of Temperature

Cawiezel and Niles (1987) also stated that the increase in temperature significantly decrease the foam viscosity up to a critical temperature of 65.6°C (150°F)

after which little change occurs. On the contrary, studies conducted by Harris and Reidenbach (1987), Khade and Shah (2004), Sani et al. (2001) show that foam viscosities do continue to decrease at temperatures above 65 °C (150 °F).

Phillips et al. (1987) and, Harris and Reidenbach (1987) comment on the decrease in high-temperature stability of CO_2 and N_2 foams, respectively. They attribute this being true due to the surfactant and gelling agent being used. Harris and Reidenbach stated that by increasing concentration of the gelling polymer agent, foam stability is not effected whereas Phillips et al. states that there is a minimum concentration of the gelling polymer agent which is required to support stable foam. Furthermore, they also indicated that stability can be further improved by increasing polymer concentration. Both studies reported that stability depends on the surfactant type and concentration.

2.9 Associated Yield Stresses

The associated yield stress is important in foam hydraulics. In the absence of wall slip, it is the minimum pressure gradient that is required for the fluid at a given shear rate for flow to occur between the two points over which the pressure gradient is measured (Cawiezel and Niles 1987). Coussot (2014) stated that yield stress and wall slip can impact the flow characteristics foams more than other types of fluids. This is discussed with more detail in Section 2.10.

Reidenbach et al (1986) studied the flow properties of CO_2 and N_2 foams at different qualities and polymer concentrations. Their data indicated that the yield point and foam consistency index for a particular texture of foam is an exponential function of quality. Using trial and error, a constant value for power law index, n was selected

following which the value of yield point, τ_y was found from a plot of wall shear stress versus nominal Newtonian shear rate (8v/d) raised to the n^{th} power on Cartesian coordinates utilizing computed solutions. As mentioned earlier, their study suggests that the rheological behavior of foams can best be described by a Herschel-Bulkley model, where the yield stress, τ_y is given by:

$$\tau_y = \alpha\Gamma \; for \; \Gamma \leq 60\% \tag{2.7}$$

$$\tau_y = \beta e^{\delta\Gamma} \; for \; \Gamma \geq 60\% \tag{2.8}$$

where α, β and δ are empirical constants that vary for CO_2 and N_2 foams but are the same for a varying liquid phases with the same gas phase. The foam consistency index as expressed by them is:

$$K_f = K_L e^{C_4\Gamma + C_5\Gamma^2} \tag{2.9}$$

Barnes and Walters (1985) hypothesized that the yield stress is just an empirical constant for representing viscosity functions over the shear rate range of measurements, and that this range does not include zero-shear rate at which the yield stress is observed normally. They indicated that accurate measurements at lower shear rates always disproves the existence of a yield stress.

Kraynik (1988) suggested that explicit methods of measuring yield-stress rely upon cases where there is no flow below a critical shear stress. The time frame of such observations and experimental sensitivity is finite making the former method a limitation. Yet he still asserts that foam does have a yield stress and bases this upon reasonable experimental evidence from other studies.

Princen (1985) also conducted measurements of the yield stress for concentrated emulsions and foams, where it is shown that the yield stress, τ_y, of foams and highly concentrated emulsions is given by:

$$\tau_y = 1.277 \left(\frac{\sigma}{R_{32}}\right) \Gamma^{1/3} F_{max}(\Gamma) \quad (2.10)$$

where σ is the interfacial tension, Γ is the volume fraction of the dispersed phase, $F_{max}(\Gamma)$ is the mean, dimensionless contribution to the yield stress, and R_{32} is the surface-volume based mean drop radius. Thus, the model does show the requirement of information regarding the structure of the foam.

2.10 Wall Slip Effect and Slip Correction

Wall slip effect is seen when fluids violate the no-slip boundary conditions of Newtonian fluid mechanics, which states the velocity of the fluid element in contact with the wall is zero. It can be detected with the use of two or more flow conduits of different diameters with identical length. When the corresponding flow data of the varying diameters is plotted on a rheogram, it should coincide in absence of wall slip. A parallel right-shifting in a data set often indicates the presence of wall slip and corrections must be made to obtain the correct rheogram.

Foams while flowing in a pipe sometimes tend to produce a thin liquid film between the pipe wall and the bulk foam, and this "slippage" results in a lower frictional loss than expected due to the lubricity of the film layer (Saintpere et al. 1999). This results in the right-shifting of flow curves in a rheogram obtained from pipe viscometers with different diameters.

Coussot (2014) also mentions that if slip were to occur for a yield stress fluid, it can flow steadily when subjected to much lower stresses than the yield stress. This type of critical behavior change should be avoided and can be done so by using rough wall surfaces, with a roughness significantly greater than the maximum size of the film thickness. Similar observations were also mentioned by Thondavadi and Lemlich (1985) in their study of foams wherein the presence of wall slip was observed while using acrylic pipes and the absence of it while using galvanized steel pipes. Stainless steel pipes have been used for this study and it is notable to mention that no wall slip was observed.

When wall slip is observed, slip correction is performed by assuming a slip velocity at the wall. The observed flow rate can be expressed as a summation of the no slip and slip flow rates as:

$$Q_{observed} = Q_{no\ slip} + Q_{slip} \tag{2.11}$$

It can then be expressed in terms of nominal Newtonian shear rates:

$$\left(\frac{8U}{D}\right)_{observed} = \left(\frac{8U}{D}\right)_{no\ slip} + \left(\frac{8U}{D}\right)_{slip} \tag{2.12}$$

where U is the average velocity.

The two main slip correction methods have been developed by Mooney (1931) and Jastrezbski (1967). Mooney's method assumes that the slip velocity depends only on the wall stress and defines it mathematically as:

$$U_{slip} = \beta\tau_w \tag{2.13}$$

where β is the slip coefficient. This is a reasonable assumption, at least for fluids without macroscopically observable structures (Enzendorfer et al. 1995). Thus, combining Eqn. (2.13) and (2.14), the following relationship can be established.

$$\left(\frac{8U}{D}\right)_{observed} = \left(\frac{8U}{D}\right)_{no\ slip} + \frac{8\beta\tau_w}{D} \tag{2.14}$$

This means that a plot of observed nominal Newtonian shear rate versus the reciprocal of pipe diameter at a fixed wall stress should result in a linear trend. The slope divided by $8\tau_w$ is the slip coefficient, β. The slip coefficient is determined for several different wall stresses, which is then plotted against the different shear stresses and a relationship is established. This is then used to correct the measurements for all the available data. Upon doing so, the original measurements can be corrected by subtracting the second term in Eqn. (2.14). Since usually the data points do not correspond exactly to the same wall stress, interpolation may be necessary.

Jastrezbski (1967) stated that fluids with macroscopic structure such as foams, the slip is the result of a more complex interaction between the wall and the fluid and suggested that the diameter of the pipe affects it. He defines slip velocity mathematically as:

$$U_{slip} = \frac{\beta_c\tau_w}{D} \tag{2.15}$$

where β_c is modified slip coefficient. Thus, combining Eqns. (2.12) and (2.15), the following expression can be obtained:

$$\left(\frac{8U}{D}\right)_{observed} = \left(\frac{8U}{D}\right)_{no\ slip} + \frac{8\,\beta_c\tau_w}{D^2} \tag{2.16}$$

According to Eqn. (2.16), a plot of the observed nominal Newtonian shear rate versus the reciprocal of the squared pipe diameter at a fixed wall stress should also result in a linear trend. The slope divided by $8\tau_w$ is the modified slip coefficient, β_c. Every given wall stresses would have a different modified slip coefficient. Thus, a relationship between the two is established and corrections are made like that mentioned in Mooney's method.

Chapter 3: Theoretical Background

3.1 Rheological Models

According to the society of rheology, rheology is defined as the science of deformation and flow of matter. A fluid will undergo continuous deformation if subjected to a shear stress. Consider a fluid that is bound by two parallel surfaces, of area A, separated by a distance H with the bottom portion held stationary (Fig. 3.1). If a force F was applied to the upper portion, it moves at a velocity, V in the direction of the force. The fluid continues to deform provided the force is applied, which is directly proportional to the area of the surface and the resultant shear stress is expressed as $\tau = F/A$. For laminar flow cases, a velocity profile $v = V*y/H$ is established within the fluid. The no-slip condition states that the fluid bounding the lower surface remains stationary and the fluid elements bound to the upper surface moves at the plate velocity, V.

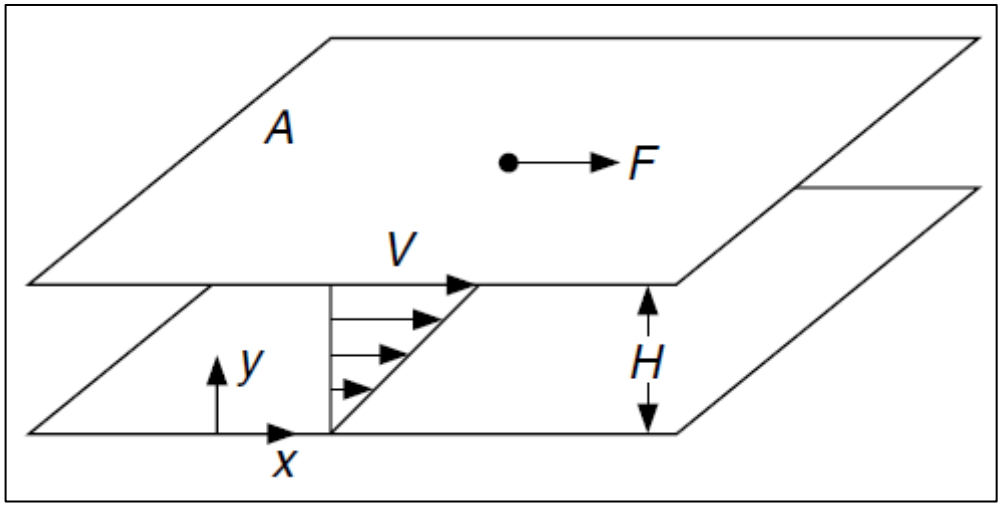

Figure 3.1 Deformation of a fluid between two surfaces subjected to a force.

The velocity gradient $\gamma = du/dy$ is called the shear rate for the flow. The ratio of shear stress to shear rate is viscosity of the fluid, μ (Tilton 2008). Fluids are described as Newtonian or non-Newtonian depending on their response to shearing. Water and mineral oil are examples of Newtonian fluid wherein the viscosity remains constant for varying shear rate. Drilling muds, drill-in fluids, drilling foams, workover and completion fluids, cement, specialty fluids are some common fluids encountered in the oilfield and they are non-Newtonian fluids wherein the viscosity varies with shear rate. Hence, for non-Newtonian fluids, the viscosity is synonymous with apparent viscosity (η) which is not constant at a given pressure and temperature. Rheology measurements are usually taken on a continual basis while drilling and adjusted with additives or dilution to meet the needs of the operation. There are four primary rheological models (Fig. 3.2), which establish the relationship between the shear rate and stress.

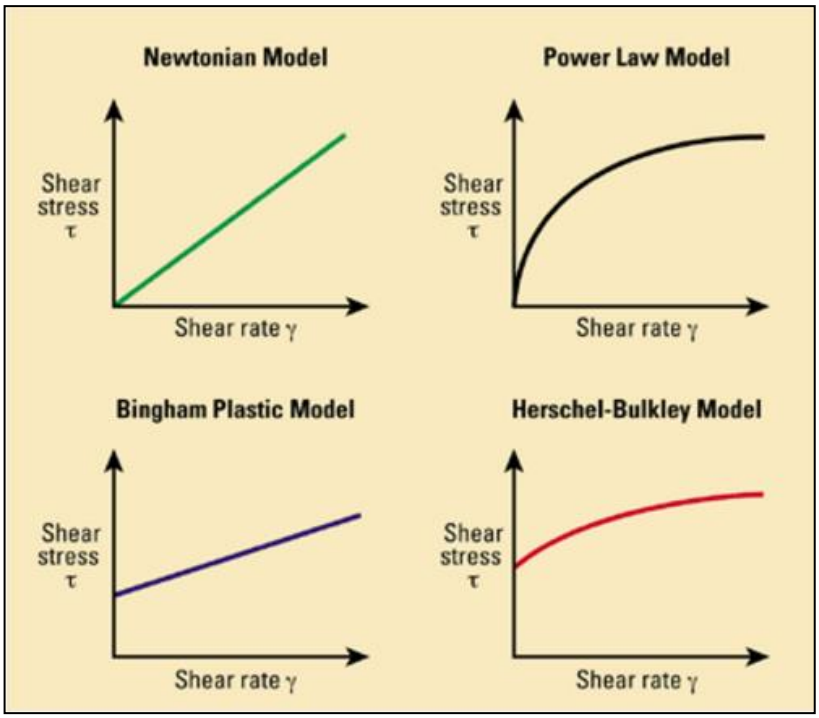

Figure 3.2 Rheological models (Source: Schlumberger Oilfield Glossary 2017)

3.1.1 Newtonian Model

For a Newtonian fluid, the viscosity is independent of shear rate. A rheogram for Newtonian fluids fluid is a straight line passing through the origin. Mathematically, it is expressed as:

$$\tau \propto \gamma \tag{3.1}$$

$$\tau = \mu\gamma \tag{3.2}$$

3.1.2 Non-Newtonian Models

As mentioned earlier, non-Newtonian fluids do not have a constant viscosity for varied shear rates but have an apparent viscosity, which is a function of the resulting shear rate. Different non-Newtonian rheological models such as Bingham Plastic, Power-Law and Herschel-Buckley (Yield Power-Law) models have been developed to describe the relationship accurately.

Power-Law Model

The power-law model (also known as Ostwald–de Waele model) uses two variable parameters to relate shear stress to the shear rate: consistency index, K and flow behavior index, n. The model in is quite useful due to its simplicity. Thus:

$$\tau = K\gamma^n \tag{3.3}$$

The apparent viscosity, η, is the ratio of shear stress to shear rate, and is given by:

$$\eta = K\gamma^{n-1} \tag{3.4}$$

The power law model is further classified based on the flow behavior index. When n less than 1, then the fluid is a shear-thinning fluid. Pseudoplastic is another terminology for fluids exhibiting such behavior wherein the apparent viscosity decreases with increasing shear rate. Rubber latex is an example of a power-law fluid.

When n is one, power-law model becomes the Newtonian model where the shear stress is directly proportional to the shear rate. The flow consistency index, K, is in this case equal to the viscosity, μ. When n is greater than one, the fluid is a shear-thickening fluid. The apparent viscosity of such a fluid increases with increasing shear rate and is also known as dilatant fluid. Quicksand is a common example.

Bingham Plastic Model

Some fluids do not flow at until a shear stress greater than the threshold stress, also known as, yield stress, τ_y. An elastic behavior similar to that of a solid is observed for shear rates which produce a shear stress less than the yield stress, following which linear Newtonian flow behavior is observed after, where the viscosity is constant. This is known as the plastic viscosity, μ_p. The shear stress-shear rate relationship is given as:

$$\tau = \tau_y + \mu_p \gamma \tag{3.5}$$

And, the apparent viscosity, η is expressed as:

$$\eta = \frac{\tau_y}{\gamma} + \mu_p \tag{3.6}$$

Herschel-Bulkley Model

It is also known as the yield power-law model. Fluids that obey the Herschel-Bulkley model also does not flow until a shear stress greater than the yield stress is attained then it exhibits power-law fluid behavior. The shear stress-shear rate relationship is given as:

$$\tau = \tau_y + K\gamma^n \tag{3.7}$$

Hence, the apparent viscosity, η is expressed as:

$$\eta = \frac{\tau_y}{\gamma} + K\gamma^{n-1} \tag{3.8}$$

3.1.3 Time Dependence Behavior of Non-Newtonian Fluids

Some non-Newtonian fluids exhibit time-dependent rheological behavior (Fig. 3.3). Time-dependent fluids are those for which the shear stress is a function of shear rate and shear rate history. These fluids are usually classified into two groups; thixotropic and rheopectic fluids. Under isothermal conditions, thixotropic fluid exhibits a reversible decrease in shear stress with time at a constant shear rate whereas rheopectic fluid shows a reversible increase in shear stress with time at a constant rate of shear.

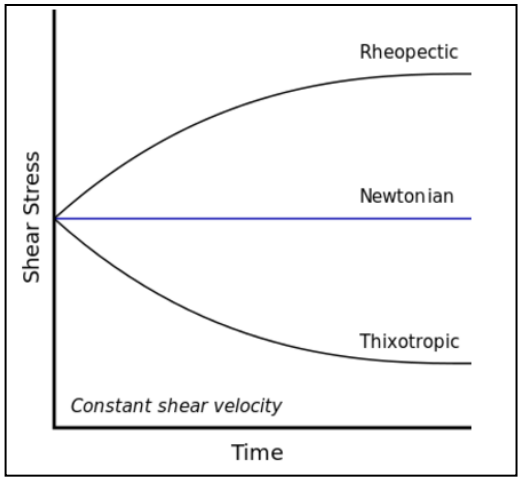

Figure 3.3 Time dependence of shear stress for non-Newtonian fluids (Source: Wikipedia.org)

3.2 Significance of Rheology Measurements

Rheograms, which give meaningful relationships between the wall shear stress, $\tau_{w,}$ and the shear rate, γ is the primary aim of any rheological study. It is a direct assessment of flowability of the material. For example, a highly viscous fluid requires more power to pump than one with low viscosity. Knowing its rheological behavior, therefore, is useful when designing systems with piping and pumping needs such as a circulation of drilling fluid in the wellbore. The viscosity of a fluid is defined as the resistance of the fluid against flow under laminar flow condition. Reynolds number, Re, is used to determine the point at which laminar flow evolves into turbulent flow. Reynolds number is a dimensionless quantity, which is the ratio of inertial forces to the viscous forces of the fluid. For a laminar flow regime, viscous forces dominate over the inertial forces and are vice-versa for a turbulent flow regime.

3.3 Rheometry

Generically, it is termed as the experimental method to evaluate the rheological properties of flowing materials. The primary aim is to establish a rheogram for the

fluid. Rheometers are used for rheometry, and in this research two types of rheometers were used, rotational and pipe viscometers.

3.3.1 Rotational Viscometer

The Couette viscometer is a common type amongst rotational viscometers and determines the viscosity by measuring the torque required to turn a suspended bob in contact with a fluid at a given shear rate (Fig. 3.4).

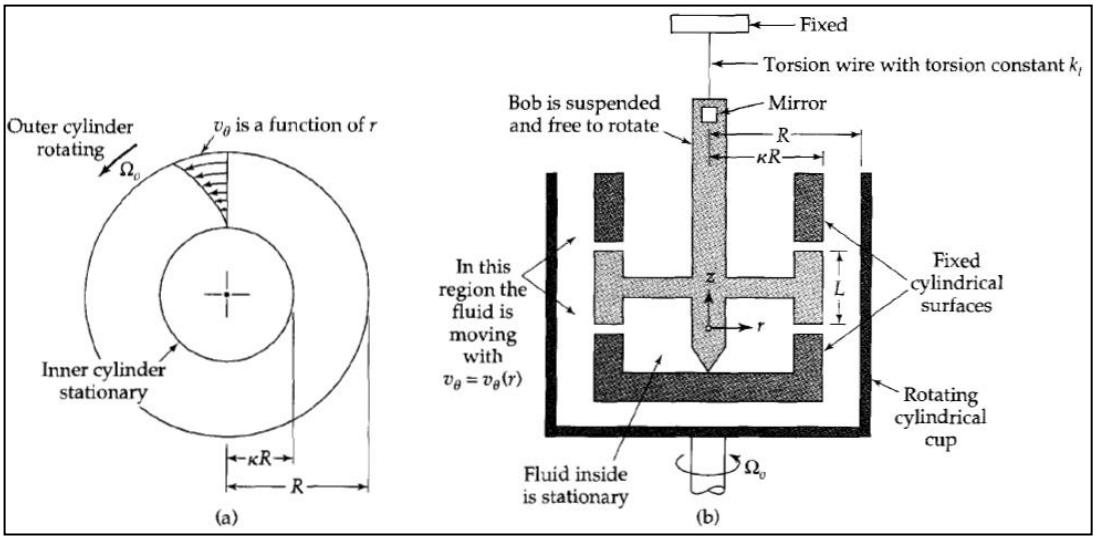

Figure 3.4 (a) Velocity flow profile inside a rotational viscometer

(b) Components of a rotational viscometer,

Source: Transport Phenomena (Bird et al. 2001)

The fluid is placed in between the cylindrical cup and suspended bob, which is then made to rotate with a fixed angular velocity, Ωo. The rotating liquid being a viscous one, causes the suspended bob to turn until the torque produced by the fluid's momentum equals the product of the torsion constant, k_t and the angular displacement, θ_b of the bob. The angular displacement is measured by observing the deflection of a dial that rotates in a synchronous manner with the rotation of the bob as in the case of Fann™ 35 and OFITE™ 900 viscometers. Measurement conditions are controlled to

ensure a steady, tangential, laminar flow in the annular space between the two coaxial cylinders of radius κR and R where κ < 1 (Bird et al. 2001). The relationship between the torque generated and the applied angular velocity is given by:

$$T = 4\pi\mu\Omega_o R^2 L\left(\frac{\kappa}{1-\kappa^2}\right) = C\mu\Omega_o \tag{3.9}$$

The torque is also related to the angular displacement, θ_b as:

$$T = k_t\theta_b \tag{3.10}$$

Eqns. (3.9) and (3.10) assume slot flow approximation for fluids in annular spaces (i.e. it assumes flow between two parallel plates) and is valid when $\boldsymbol{\kappa > 0.3}$. Correction factors must be considered if the former is not valid. Therefore, the angular velocity of the cup and the resultant deflection of the bob is used to determine the viscosity. For Newtonian fluids, this is the actual viscosity of the fluid and for non-Newtonian fluids; this is the apparent viscosity of the fluid at an angular velocity of Ω_o.

3.3.2 Pipe Viscometer

Pipe viscometers show better reliability and accuracy than rotational viscometers, as the slot flow approximation is not needed since the flow is measured inline through pipes. On being relatively expensive and not convenient for field applications, its use is commonly restricted for research purposes and in-line viscosity measurements. A standard pipe viscometer system has flow rate and pressure loss measuring instrumentations. To obtain reliable and accurate measurements, these types of viscometers must have sufficiently long entrance and exit sections to allow sufficient distance for fully developed laminar flow conditions in the test section (Fig. 3.5).

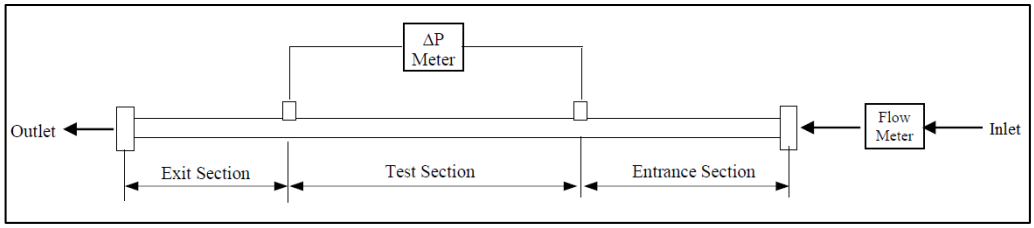

Figure 3.5 Typical pipe viscometer System (Ahmed and Miska 2009)

To analyze the viscometric flow, consider a short segment in the test section of the viscometer with diameter, D (radius, R) and length, ΔL (Fig. 3.6). In this case, the flow rate through the segment is calculated from the velocity profile as:

$$Q = 2\pi \int_0^R v(r) r dr \tag{3.11}$$

where v(r) is the axial velocity.

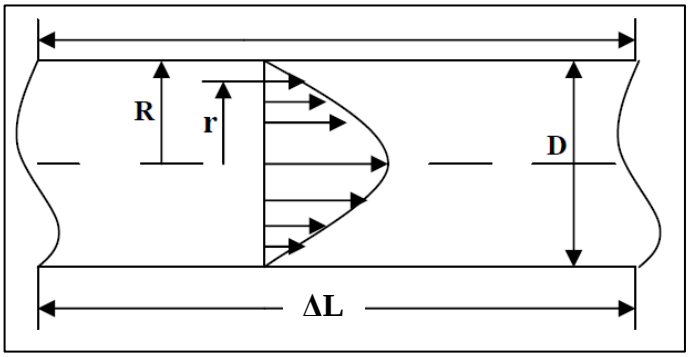

Figure 3.6: Fluid flow in a segment of the test section (Ahmed and Miska 2009)

Applying integration by parts and the boundary condition v(R) = 0, the following expression can be obtained for flow rate:

$$Q = -\pi \int_0^R r^2 \frac{dv}{dr} dr \tag{3.12}$$

For a steady state flow with constant density, the momentum balance at radius R over a length of ΔL yields:

$$\tau_w = \frac{R\Delta P}{2\Delta L} \tag{3.13}$$

where, τ_w is the wall shear stress. Similarly, shear stress at any radius r is expressed as:

$$\tau(r) = \frac{r\Delta P}{2\Delta L} \tag{3.14}$$

Therefore:

$$\frac{\tau\,(r)}{r} = \frac{\tau_w}{R} \tag{3.15}$$

Changing the variables:

$$r = \frac{\tau\,(r)}{\tau_w} R \rightarrow dr = \frac{R}{\tau_w} d\big(\tau\,(r)\big) \tag{3.16}$$

Plugging into Eqn. (3.12), the following expression can be obtained:

$$Q = -\pi \int_0^{\tau_w} \left(\frac{\tau\,(r)}{\tau_w} R\right)^2 \frac{dv}{dr} \frac{R}{\tau_w} d\big(\tau\,(r)\big) \tag{3.17}$$

After rearrangement:

$$Q = -\pi \int_0^{\tau_w} \left(\frac{R}{\tau_w}\right)^3 \tau^2 \, \frac{dv}{dr} d\tau \tag{3.18}$$

The shear rate, $-\boldsymbol{\frac{dv}{dr}}$ is a function of the shear stress, τ or mathematically,

$$f(\tau) = -\frac{dv}{dr} \tag{3.19}$$

Thus:

$$\frac{Q}{\pi R^3} = \left(\frac{1}{\tau_w}\right)^3 \int_0^{\tau_w} \tau^2 f(\tau) d\tau \tag{3.20}$$

$$\frac{Q{\tau_w}^3}{\pi R^3} = \int_0^{\tau_w} \tau^2 f(\tau) d\tau \tag{3.21}$$

Differentiating with respect to τ_w using Leibniz Integral rule yields:

$$\frac{3{\tau_w}^2 Q}{\pi R^3} + \frac{{\tau_w}^3}{\pi R^3}\frac{dQ}{d\tau_w} = {\tau_w}^2 f(\tau_w) \tag{3.22}$$

After rearrangement:

$$f(\tau_w) = \frac{3Q}{\pi R^3} + \frac{\tau_w}{\pi R^3}\frac{dQ}{d\tau_w} \tag{3.23}$$

It is known that the average velocity through a flow segment is flow rate divided by the cross-sectional area. Thus:

$$U = \frac{Q}{\pi R^2} \rightarrow \frac{2U}{D} = \frac{Q}{\pi R^3} \tag{3.24}$$

The shear rate at the wall is related to the wall shear stress according to Eqn. (3.25). Therefore:

$$\gamma_w = -\left(\frac{dv}{dr}\right)_{\tau_w} = \frac{3}{4}\left(\frac{8U}{D}\right) + \frac{\tau_w}{4}\frac{d\left(\frac{8U}{D}\right)}{d\tau_w} \tag{3.25}$$

Eqn. (3.25) can be expressed using the logarithmic plot gradient (flow behavior index) as:

$$\gamma_w = \frac{1}{4}\left[\frac{3N+1}{N}\right]\frac{8U}{D} \tag{3.26}$$

where N is flow behavior index, which is defined as:

$$N = \frac{d(ln(\tau_w))}{d\left(ln(\frac{8U}{D})\right)} \tag{3.27}$$

Pipe viscometer data is normally plotted in terms of the logarithm of wall shear stress versus the logarithm of nominal Newtonian shear rate (8U/D) as shown in Fig. 3.7. The flow behavior index, N is the slope of the plot at a given shear stress.

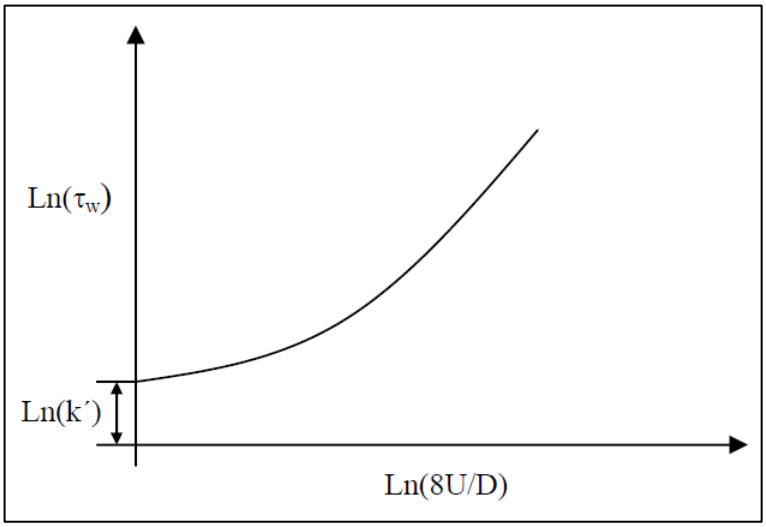

Figure 3.7 Logarithmic plot of wall shear stress versus nominal Newtonian shear rate (Ahmed and Miska 2009)

where k' is the generalized flow consistency index used to express the constitutive equation in form of the generalized power law model as:

$$\tau_w = k'\left(\frac{8U}{D}\right)^N \tag{3.28}$$

If the logarithm of wall shear stress versus logarithm of nominal Newtonian shear rate plot forms a straight line, it is a power law fluid as the flow behavior index is constant. Then, Eqn (3.28) gives:

$$\tau_w = K{\gamma_w}^n = K\left[\left(\frac{3n+1}{4n}\right)\frac{8U}{D}\right]^n \tag{3.29}$$

Equation (3.30) is valid only for laminar flow in which the Reynolds number is greater than the critical Reynolds number. The generalized Reynolds number, Re is related to the wall shear stress using the following equation.

$$Re = \frac{8\rho U^2}{\tau_{w,lam}} \tag{3.30}$$

where $\tau_{w,lam}$ is wall shear stress obtained from the laminar flow equation (Eqn. 3.30). The fanning friction factor of pipe flow is expressed as:

$$f = \frac{\tau_w}{0.5\rho U^2} \tag{3.31}$$

For power law fluid, Eqns. (3.30) and (3.29) can be combined to obtain the following expression:

$$Re = \frac{8\rho U^2}{K\left[\left(\frac{3n+1}{4n}\right)\frac{8U}{D}\right]^n} = \frac{8^{n-1}\rho U^{2-n}D^n}{K\left[\left(\frac{3n+1}{4n}\right)\right]^n} \tag{3.32}$$

3.4 Foam Quality and Density

The foam quality, Γ of given foam is defined as the gas fraction of the foam at the corresponding pressure and temperature and is given as:

$$\Gamma = \frac{Gas\ Volume}{Gas\ Volume + Liquid\ Volume} \tag{3.33}$$

In this study, density of foam, $\rho_{foam,}$ is measured in-line using a flow meter. Hence, at a given pressure and temperature, it is related to the quality as follows:

$$\rho_{foam} = \rho_{gas}(\Gamma) + \rho_{liq}(1 - \Gamma) \tag{3.34}$$

After rearranging, foam quality is the foam quality is expressed as a function of its density and densities of gas and liquid phases:

$$\Gamma = \frac{\rho_{liq} - \rho_{foam}}{\rho_{liq} - \rho_{gas}} \tag{3.35}$$

At high-pressures, the density of gas changes significantly as compared to that at low pressures. The ideal gas law is applied to get the gas density at test pressure and temperature.

$$\rho_{gas} = \frac{P.T_{STP}}{P_{STP}.T} \cdot \rho_{gas\_STP} \tag{3.36}$$

where P is test pressure, T_{STP} is the temperature at standard conditions, P_{STP} is the pressure at standard conditions, T is the test temperature and ρ_{gas_STP} is the density of the gas at standard conditions. The compressibility factor, z for the tests that are conducted in this research vary from 0.99 to 1.02, and is thus, assumed to be equal to 1.

Chapter 4: Experimental Studies

Aqueous foams were tested to see the influence of pressure on rheology at ambient temperature of 23.9°C (75°F). Polymer-based foams were tested to study the effect of temperatures on rheology at 6.9 MPa. Data is acquired using VBA in Excel from the sensors using a data acquisition board. The measurements collected include differential pressures across the foam generation section and test section, overall system pressure, flowrate, density and temperature. An anionic foaming agent (Howco Suds™) was used as the surfactant for both foams and the concentration was 2% by volume.

4.1 Test Matrix

This research was carried out with two kinds of foams: aqueous foams and polymer foams. Tables 4.1 and 4.2 describe formulations of the foams, and test variables and their range.

Table 4.1: Foam formulation and test variables - Aqueous foams

Foam type	Aqueous foam		
Pressure (MPa)	6.89	13.79	20.68
Temperature (°C)	23 ± 1%	23 ± 1%	23 ± 1%
Liquid Phase	Water		
Gaseous Phase	Nitrogen		
Surfactant used	Howco-Suds™ Foaming Agent		
Conc. of Surfactant (vol. %)	2%		
Foam Qualities (%)	40 - 80 %	55 - 75 %	55 - 75%
Increments of foam qualities (%)	5%	10%	10%

Table 4.2: Foam formulation and test variables - Polymer-based foams

Foam type	Polymer-based foam		
Pressure (M Pa)	6.9	6.9	6.9
Temperature (°C)	23 ± 2	76 ± 2	107 ± 2
Liquid Phase	Water + 0.25% PAC (by wt.)		
Gaseous Phase	Nitrogen		
Surfactant used	Howco-Suds™ Foaming Agent		
Conc. of Surfactant (vol.%)	2%		
Foam Qualities (%)	45 - 75 %	45 - 75 %	45 - 75 %
Increments of foam qualities (%)	10%	10%	10%

Water and nitrogen in the presence of the Howco-Suds™ foaming agent were used to generate the aqueous foams. These foams were tested only at high pressure as they were unfit for high temperature tests due to their instability.

Poly Anionic Cellulose (PAC) available in the market (POLYPAC-R) was used to create polymer-based foams. The polymer was first mixed with water and then left to hydrate for 24 hours, then combined with nitrogen in the presence of the foaming agent to generate the desired quality foam.

4.2 Experimental Setup

The experimental setup (Fig. 4.2) is developed to generate stable foam under high-pressure (maximum 27 MPa) high-temperature (maximum 175°C) conditions and perform rheology tests using different diameter pipe viscometers. The flow loop (Fig. 4.1) consists of: i) a 1000-mL base liquid tank, used as an entry point for the liquid phase into the system; ii) stainless steel tubing and fittings rated for appropriate high pressures and high temperatures; iii) stainless needle valves for regulating flow and generating foam; iv) a variable speed gear pump (Micropump GA-T23) capable of pumping fluid at a maximum flow rate of 1.14 L/min and handling multiphase flow

(Fig. 4.3); v) a high-pressure gas-supply cylinder that contains nitrogen at 41.4 MPa (6000 psi); vi) double-pipe heat exchangers that are connected to an air-cooled chiller and electric heater; vii) a foam generation section (Fig. 4.4) with a needle valve that induces shearing and use pressure energy for foam generation and static mixers installed upstream and downstream of the valve for maintaining homogeneity of the foam; viii) a Coriolis flow meter (Endress Hauser Promass 83 A), which measures density, flow rate and temperature; ix) three test sections having inner diameters of 3.048 mm, 6.223 mm and 12.573 mm (0.120 in., 0.245 in. and 0.495 in.); xi) differential pressure transmitters (Endress Hauser Deltabar PMD75), which measure pressure drop across the test section; and xii) a data acquisition board which is linked to a VBA program and spreadsheet for monitoring and recording test parameters.

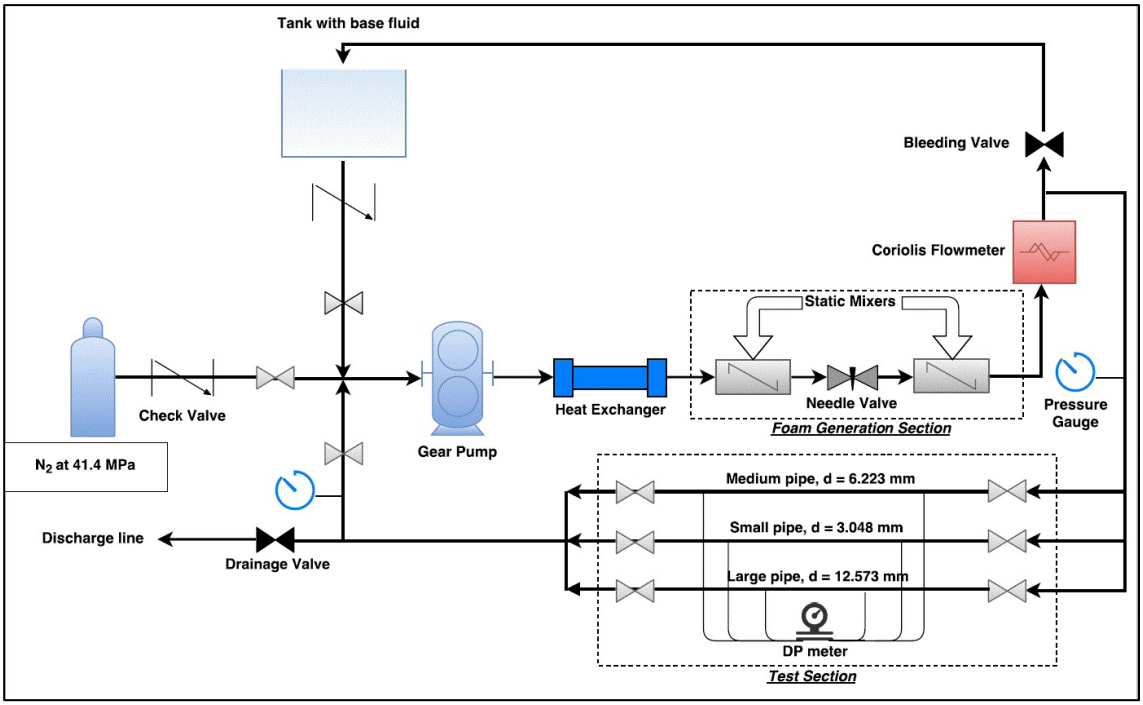

Figure 4.1 Process flow diagram of the experimental setup

The chiller that utilizes ethylene glycol to maintain ambient temperature conditions, which would otherwise increase due to viscous heating and heater, utilizes Dynalene HT as a heating fluid for maintaining high temperature in the loop.

Figure 4.2 Experimental setup

Figure 4.3 Gear pump

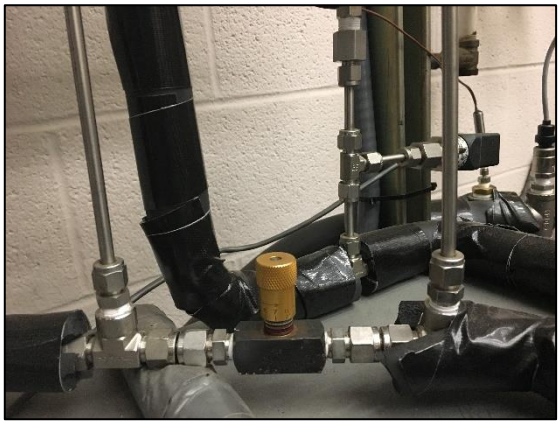

Figure 4.4 Needle valve used for foam generation

4.3 Test Procedure

First, the base fluid enters the system from the base liquid tank via a bonnet needle valve a check valve that prevents backflow to the tank. The gear pump is used to fill the loop with incoming base liquid. Then, with the help of a pressure regulator and a bonnet needle valve, the gas-supply cylinder is used to inject nitrogen to the system at the desired pressure . A check valve is also in place to prevent any backflow from the system. A needle valve located downstream of the pump used as the foam generating valve with static mixers located downstream and upstream of it to ensure homogeneity of the foam. Foam is generated by throttling the needle valve to the desired pressure drop for foam generation. The pressure drop across the needle is controlled by the level of throttle and is monitored by a differential pressure transmitter. Fluid then passes through a Coriolis flow meter to measure mass flow rate, foam density and temperature before the test section. The homogeneity of foam is established when there are stable, consistent density measurements from the flowmeter. Foam was circulated at the desired flow rate and quality to get each flow measurement and differential pressure across the test section was measured.

4.3.1 Foam Generation and Quality Control

Before beginning the foam generation process, the loop must only be filled with base fluid and all air pockets must be removed. This was performed by flowing the base liquid in an open loop configuration, in which the fluid was discharged out the system through the drainage valve and circulated back to the base liquid tank to re-enter the system. This aids in the venting of air. During the process, noticeable air bubbles were seen in the transparent return line and in the tank as they were vented to the

atmosphere. Special care should be taken to ensure that the return line is immersed within the fluid in the tank to monitor the air bubbles. The venting of air continued till there were no noticeable air bubbles in the return lines after which, the system was switched to a closed loop configuration. This was conducted so that pure nitrogen can be fed as the gas phase for foam generation and a closed loop configuration ensures no communication with the external atmosphere and allows safe pressurization of the system.

To generate foam, nitrogen was injected into the system from a pressurized cylinder via a regulated bonnet needle valve while the base fluid was recirculated by the gear pump and slowly discharging base liquid from the loop. Due to circulation through the static mixers and needle valve, nitrogen was mixed with base liquid to generate foam. The needle valve was throttled to maintain the required pressure drop (248.8 to 298.6 kPa) for foam generation.

The pressure regulator on the cylinder was used to set the test pressure in the loop. Foam quality is a function of base liquid volume in the loop. The desired quality was maintained by injecting the gas pressure while carefully draining liquid or foam out of the loop.

4.3.2 Determination of Fluid Rheology

Newtonian shear rates along with the wall shear stresses are used to obtain the rheology of a given non-Newtonian fluid. This was done by measuring the pressure drop across the viscometer while varying flow rate and viscometer sections. Then the measured data is converted into wall shear stresses and nominal Newtonian shear rates. Pressure drop readings and all other measurements for a given flow rate were taken over

ten time steps; a time step is defined as the time it takes to record one set of measurements for all test parameters by the computer system. This was done to check for reliability and consistency of the measurements. The pressure drop was measured using two differential pressure transmitters with different measurement ranges, one measuring from 0 to 10 KPa and the other from 0 to 300 KPa. The former is more accurate for low-pressure measurements and the latter provides measurements over a wide range of values.

As previously mentioned in Section 3.2, it is imperative that fully developed laminar flow is established before measuring rheology. Entry length of approximately 50 times the pipe diameter is maintained in the test sections to ensure fully developed flow. While measuring foam rheology at lower flow rates, foam properties especially its quality change because of gravity drainage and coalescence. Hence, to maintain uniform level foam generation at different test flow rate, the foam was regenerated at the maximum flow rate (0.55 L/min) for a period of 60 seconds before each flow measurement was taken (Fig. 4.5).

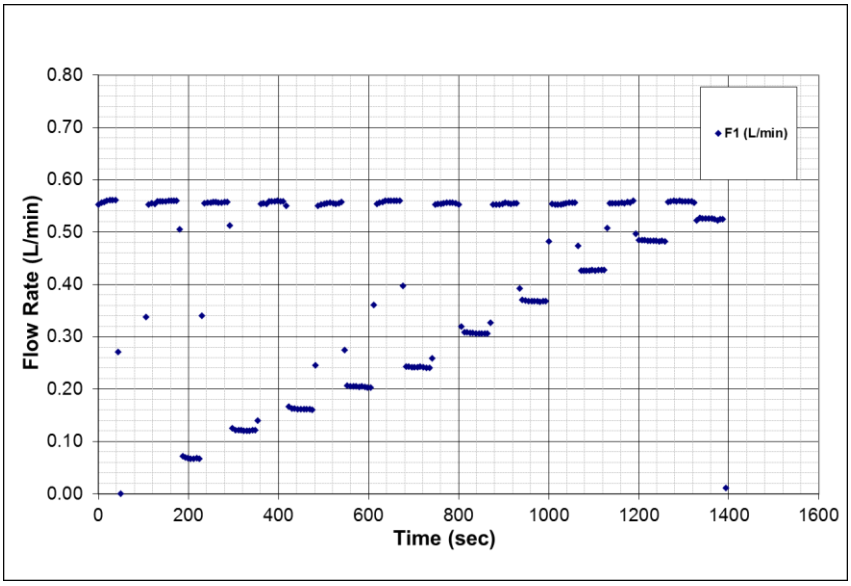

Figure 4.5 Foam being regenerated at higher flow rates before each test measurement

4.3.3 Measuring Yield Stresses

Yield stress is important characteristic of drilling fluids that they are able to flow only if they are subjected to a stress above some critical value. Otherwise, they deform in a finite way like solids. It is a challenging task to determine the critical value at which flow begins for evaluating the yield stress behavior of fluid. In this study, the presence of yield stress was evaluated during static conditions after dynamically flowing the fluid and then gradually coming to a rest. The pressure drops across the test viscometer section and foam generator were measured for the transition from the dynamic to static flow conditions. This was performed by slowly bringing the pump to stop after a set of rheology measurements in which the foam was continuously sheared. For a fluid without yield stress, the pressure drop across the viscometer would reduce to the zero value, which corresponds to no flow but in the case of a yielding fluid, there would be a significant pressure drop over a period, which when analyzed after

measurements would either reach a peak value or stay at a plateau when plotted against time.

4.4 Viscometer Validation

The recirculating pipe viscometer measurements were validated by comparing with measurements obtained from rotational viscometer (OFITE 900) at the same temperature. Tests were conducted using Newtonian mineral oil (Drakeol® 10 LT MIN OIL NF) at 23.9°C (75°F). All tests were conducted under laminar flow condition in which the Reynolds number was less than 2100. Measurements obtained from pipe viscometers with different diameters form a single flow curve on shear stress versus shear rate plot (Fig. 4.6), indicating absence of wall slippage. Beside this, the rotational viscometer measurements perfectly coincide with those of pipe viscometers. Thus, coinciding rheograms from the pipe viscometers and a standardized rotational viscometer validate pipe viscometer measurements. A slope of 0.033 Pa.s (33 cP) is inferred with the straight line passing through the origin.

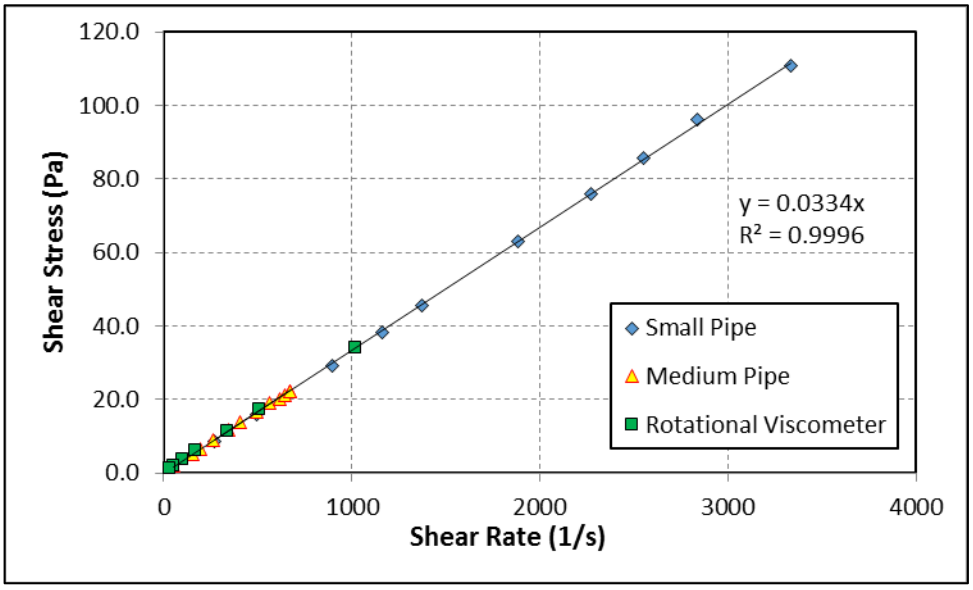

Figure 4.6 Rheograms obtained from pipe and rotational viscometers

4.5 Investigating Degradation of PAC

Polymeric fluids often degrade when exposed to high temperature and high shear rate. To assess the impact of degradation on the rheology measurement, tests were conducted on polymer-based foams under high temperature despite PAC polymer specifications citing stability of up to 148.9°C (300°F). The degradation study was performed by testing rheology of base liquid using rotational viscometer before and after foam rheology experiments. The fluid preserved its original rheological properties (Fig. 4.7) after exposure to high temperature (107°C) and high shear rate occurring in the foam generator. Thus, PAC is stable at temperatures and shear rates considered this investigation.

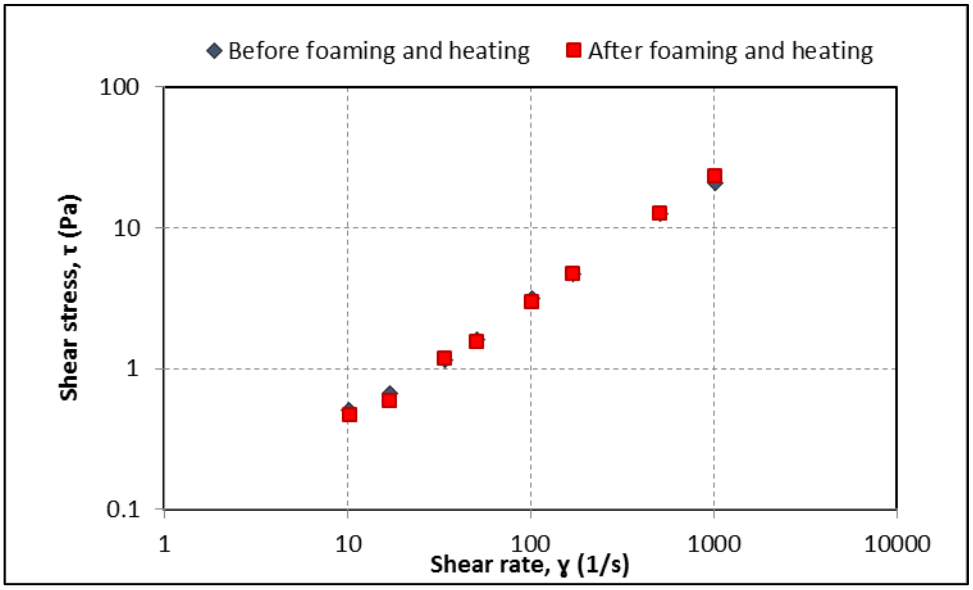

Figure 4.7 Rheogram of polymer base fluid (0.25% PAC + Water) before and after high temperature foam rheology experiments

Chapter 5: Results and Discussion

5.1 Rheology Measurements

Every rheological test aims to determine the relationship between the wall shear stress and shear rate by plotting the respective data on a rheogram. According to Eqn. (3.13), the wall shear stress, τ_w is related to the measured pressure drop (ΔP_m), diameter (D) and length (ΔL) of the test section as: $\tau_w = \frac{D}{4}.\frac{\Delta P_m}{\Delta L}$. The nominal Newtonian shear rates (γ) is related to mean velocity (U) computed from measured flow rate and pipe diameter (D). Thus: $\gamma = \frac{8U}{D}$.

5.2 Verification of Flow Regime

All tests were conducted in under laminar flow conditions having a Reynolds number less than 2100. The maximum Reynolds number during the test was 1694. The generalized Reynolds number for foam flow *in* a pipe is calculated using Eqn. (3.32) as:

$$Re = \frac{D^n U^{2-n} \rho_{foam}}{8^{n-1} K \left(\frac{3n+1}{4n}\right)^n} \tag{5.1}$$

The actual fanning friction factor (f) for foam is defined as the ratio of the wall shear stress computed from measured pressure loss (using Eqn. 3.31) to product of density and mean velocity head. Thus:

$$f = \frac{\tau_w}{\rho_{foam}.\frac{U^2}{2}} = \frac{\frac{D}{4}.\frac{\Delta P}{\Delta L}}{\rho_{foam}.\frac{U^2}{2}} = \frac{D\Delta P_m}{2\Delta L \rho_{foam} U^2} \tag{5.2}$$

As mentioned earlier, the slope and intercept of a logarithmic plot of wall shear stress versus nominal Newtonian shear rate of a power law fluid are n and $Log(\left(\frac{3n+1}{4n}\right)^n * K)$,

respectively. These values are then used to back calculate the wall shear stress for a given shear rate, which is then further used to determine the Reynolds number. The corresponding fanning friction factor is then, compared with the theoretical friction factor for a laminar pipe flow.

$$f = \frac{16}{Re} \tag{5.3}$$

As a sample case, the verification of friction factors for 75% foam quality in the small pipe is as shown in Fig. 5.1.

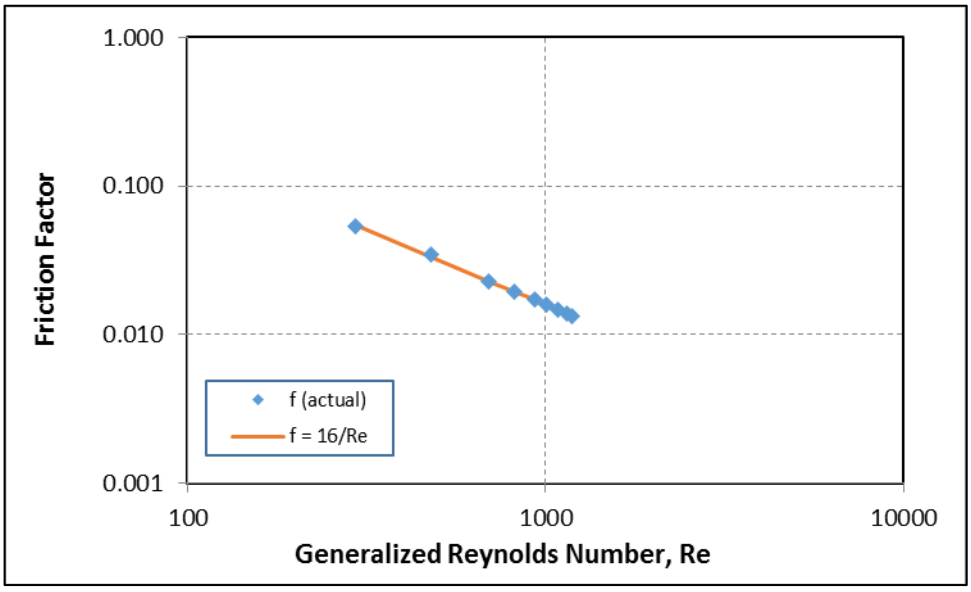

Figure 5.1 Fanning friction factor versus generalized Reynolds number

The results obtained from the pipe viscometer are presented in the next section. As mentioned in Section 4.1, two types of foams were tested; aqueous foams and polymer based foams. Since, the conditions at which the tests were performed were different; the results of the foams are discussed separately.

5.3 Aqueous Foams

The liquid phase, also referred as 0% quality foam, is mostly water and thus, the viscosity and density of the liquid phase is taken to be that of water at specified conditions. The effect of varying pressure for foams at different qualities is the primary aim of this part of the study.

5.3.1 Rheological Analysis

Tests were conducted at different pressures (6.89 13.79 and 20.68 MPa) and ambient temperature of 23.2 °C (74 °F) varying foam quality from of 40 to 80% with increments of 5%. Temperature variation was within ± 1%. The rheograms obtained from these experiments are shown in Fig. 5.2. Results demonstrate power-law relationship between wall shear stress and nominal Newtonian shear rate. The slope and intercept of measurements were computed for each foam to obtain the power law parameters to generate grey lines, which represent regression lines.

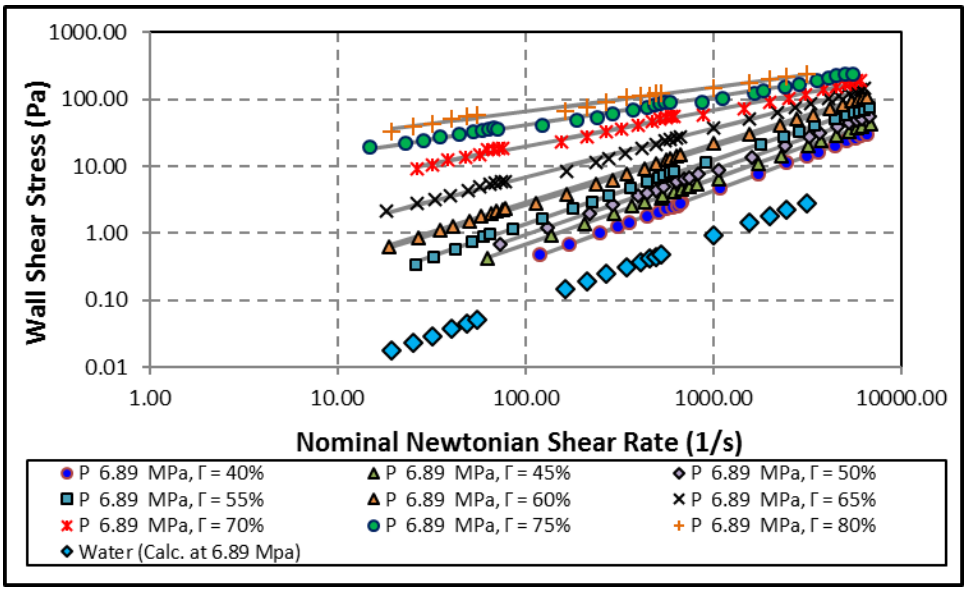

Figure 5.2 Rheogram for aqueous foams at 6.89 MPa (1000 psig) and 23.8°C (75 °F)

For a given shear rate, it is seen that the shear stress increases for increasing foam quality and this is indicative of the fact that as foam quality increases so does its apparent viscosity (Eqn. 3.4). This is articulated in the Fig. 5.3

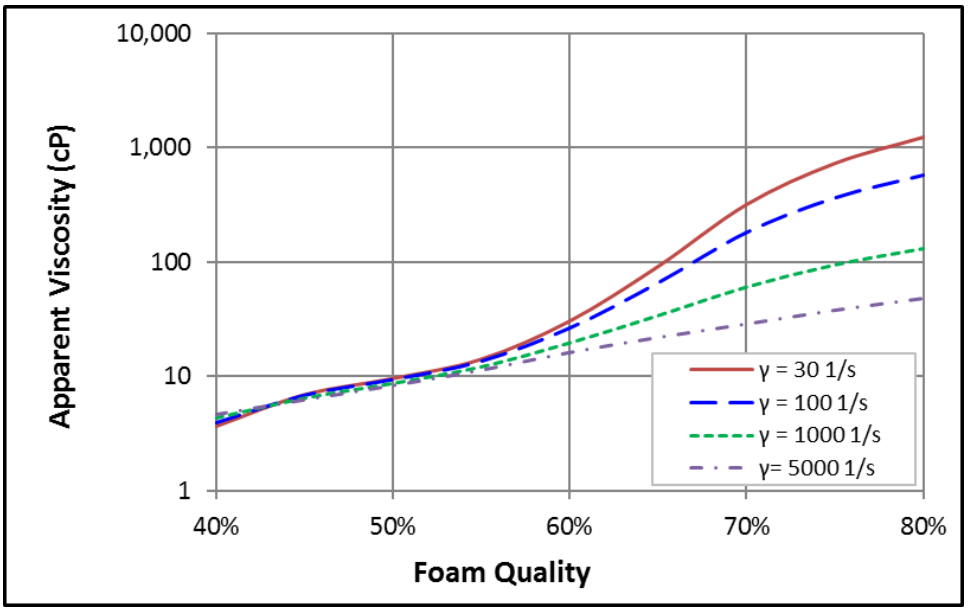

Figure 5.3 Apparent viscosity vs. foam quality for varying shear rates at 6.89 MPa (1000 psig) and 23.8 °C (75 °F)

At low qualities (40 - 55%), the apparent viscosity increases with quality but does not vary much with shear rate for a given quality. For foam qualities of 55% and above, there is a notable difference between the apparent viscosities for a given quality for increasing shear rates and an increase in magnitude of apparent viscosity is also seen from 55% onwards for given shear rates. As mentioned in Section 3.4.2, the slope of the rheogram on a log-log plot gives the power-law index, n. Water being Newtonian fluid has a power-law index of 1. For higher foam qualities, it observed from Fig. 5.2 the slope decreases (i.e. it goes further away from 1 and towards 0).

Thus, strengthening of non-Newtonian behavior was observed at high foam qualities wherein the difference in magnitude for apparent viscosity for increasing shear rates varies considerably. This can be attributed to the development of foam structure as mentioned by Ahmed et al. (2003) and Hutchins and Miller (2005). As there isn't a significant difference in the apparent viscosity of foams having quality ranging from 40 – 55% and also is not commonly used qualities for underbalanced drilling purposes, hence, foam qualities of 55%, 65% and 75% were the ones studied at higher pressures of 13.79 and 20.68 MPa (2000 and 3000 psig). The rheograms for these foams are as shown in Figs. 5.4 and 5.5.

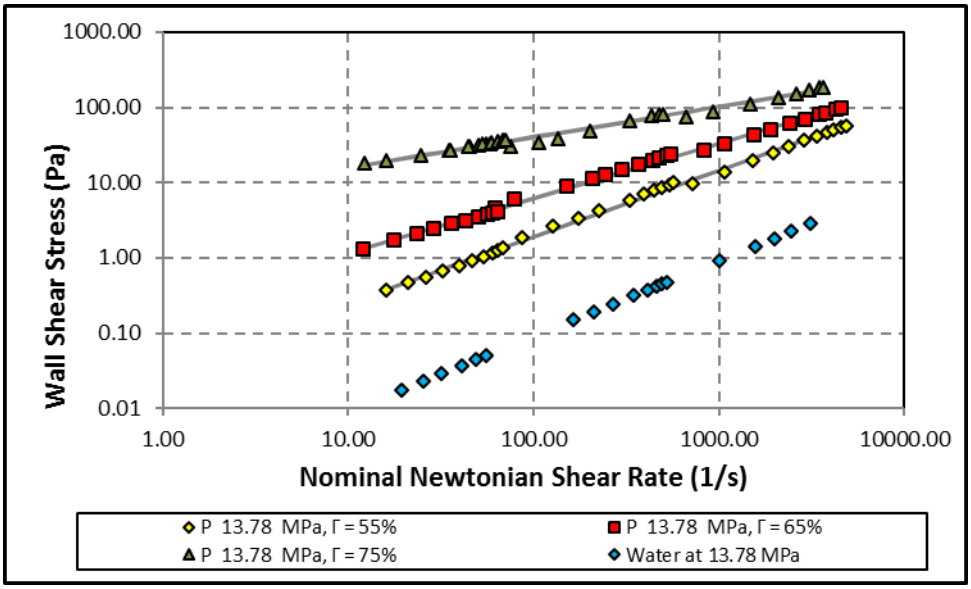

Figure 5.4 Rheogram for aqueous foams at 13.78 MPa (2000 psig) and 23.2 °C (75 °F)

Upon comparing the rheograms of 55 to 75% quality foams at different pressures and ambient temperature, there is no significant influence of pressure on foam rheology (Fig. 5.6) at constant pressure (i.e. no significant seconding effect of pressure on rheology). The rheograms of respective qualities quite closely superimpose each

other implying that changing pressure does not have substantial effect on foam rheology unlike the influence of foam quality.

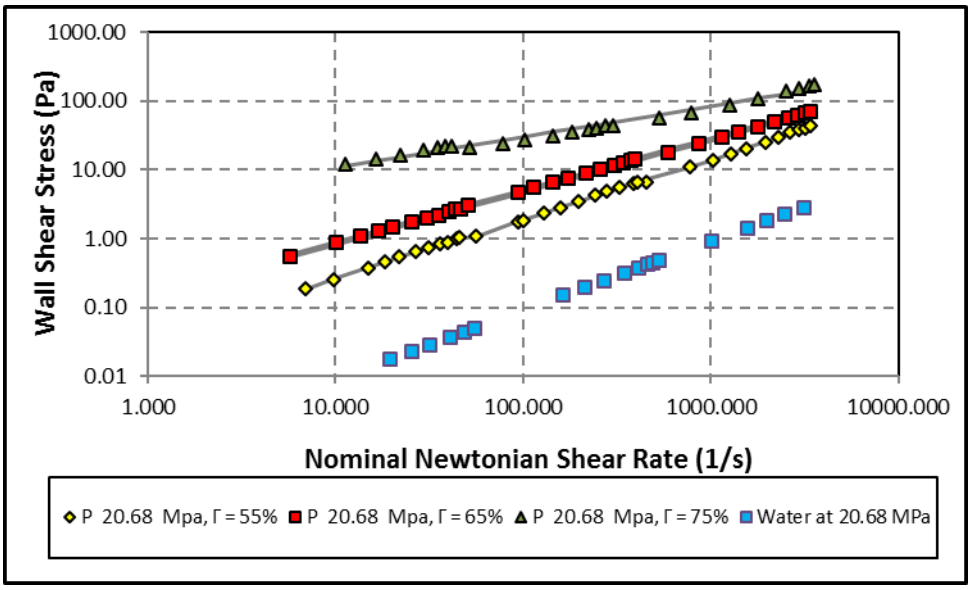

Figure 5.5 Rheogram of aqueous foams at 20.68 MPa (3000 psig) and ambient temperature of 23.8°C

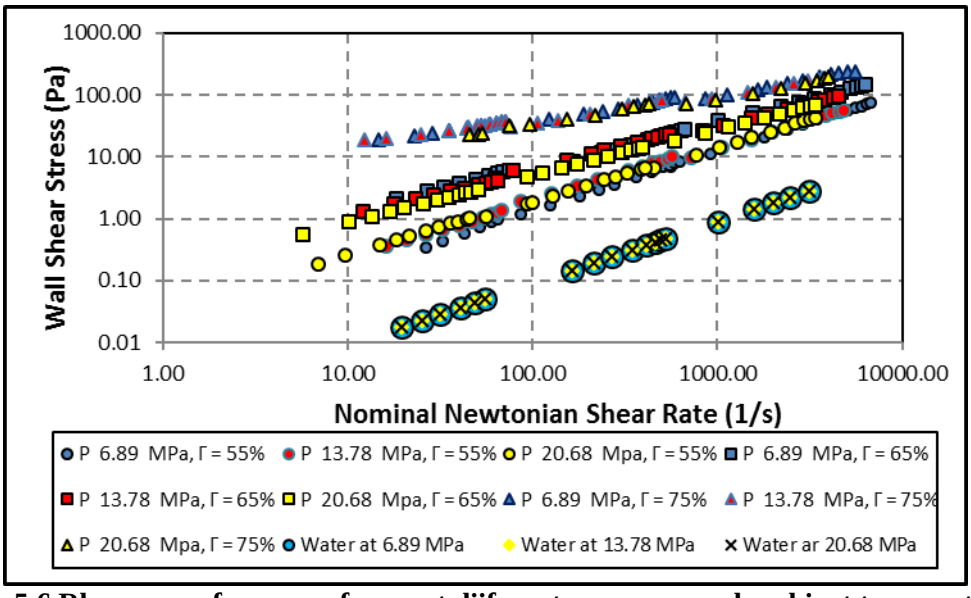

Figure 5.6 Rheogram of aqueous foams at diiferent pressures and ambient temperature of 23.8°C (75°F)

5.3.2 Correlation of Power Law Parameters

An unequivocal conclusion, which can be made from the rheograms presented in Section 5.3.1 is that, foam quality is a parameter, which is much more closely related to the rheological properties of foam as compared to pressure. Thus, making it imperative to have relationships between foam quality and power law parameters of foam, n_F and K_F. On applying curve fitting methodologies, correlations are developed relating foam quality to $1/n_F$ and K_F/K_L, where K_F is the foam consistency index and K_L is base liquid consistency index. At constant foam quality, there is no significant relationship between pressure and foam quality; therefore, only rheology measurements obtained at 6.89 MPa (1000 psig) are considered in the analysis. Table 5.1 presents the values of $1/n_F$ and K_F/K_L for aqueous foams at different qualities. The equation correlating the power-law index $1/n_F$ with foam quality, Γ is given by:

$$\frac{1}{n_F} = y_0 + \frac{a}{\left(1+\exp\left(-\frac{(\Gamma - x_0)}{b}\right)\right)} \tag{5.4}$$

where a, b, y_0 and x_0 are dimensionless constants.

Table 5.1 Values of 1/nF and KF/KL for aqueous foams

Γ	**$1/n_F$**	**K_F/K_L**
40%	0.957	3.174
45%	1.022	7.494
50%	1.030	10.665
55%	1.046	16.555
60%	1.142	46.680
65%	1.388	236.647
70%	1.886	1569.688
75%	2.367	5172.190
80%	2.730	10589.650

The dashed curve in Fig. 5.7 shows the plot of the correlation (Eqn. 5.6) relating the power-law index and quality of aqueous foams. A good match between the correlation and measurements is is observed. Thus, Eqn. (5.4) is a suitable correlation for predicting power law exponent of aqueous foam was quality ranging from 40 to 80%. The values of correlation parameters are as shown in Table 5.2.

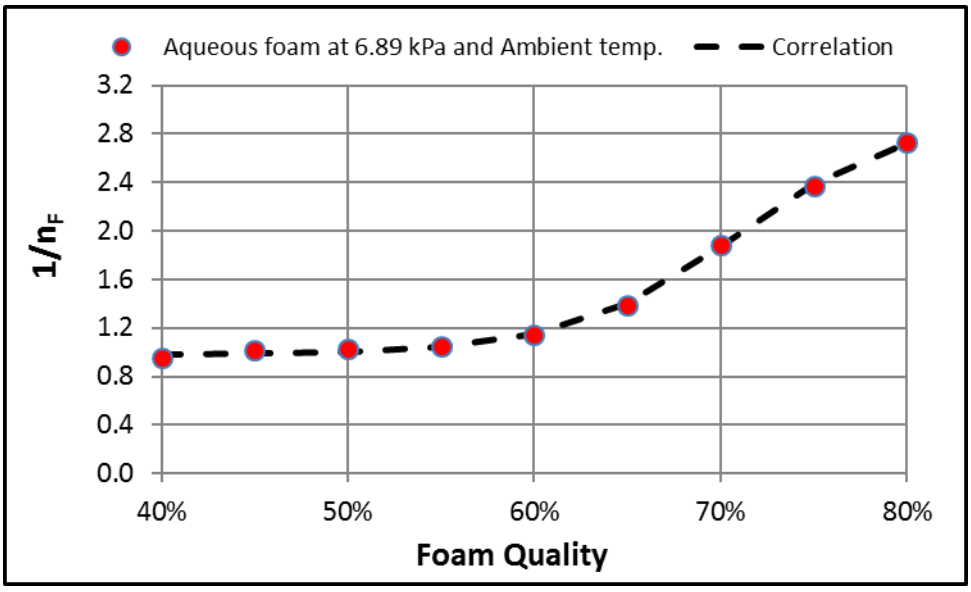

Figure 5.7 $1/n_F$ vs. foam quality for aqueous foams at 6.89 MPa (1000 psig) and 23.8°C (75°F)

Table 5.2 Dimensionless constants used in Eqn. (5.4)

Parameter	$1/n_F$
a	1.9798
b	0.0454
x_0	0.7099
y_0	0.9832

Similarly, the equation that relates the ratio of the consistency indexes (K_F/K_L) to foam quality is given by:

$$\frac{K_F}{K_L} = exp\left[y_0 + \frac{a}{(1+\exp\left(-\frac{(\Gamma - x_0)}{b}\right)}\right] \tag{5.5}$$

Figure 5.8 compares predictions of Eqn. (5.5) with measurements. Except 40% quality foam, satisfactory agreement between predictions and measurements is observed. Thus, Eqn. (5.5) is a valid for aqueous foam with quality ranging from 45 to 80%. The values of dimensionless constants (a, b, y_0 and x_0) are presented in Table 5.3.

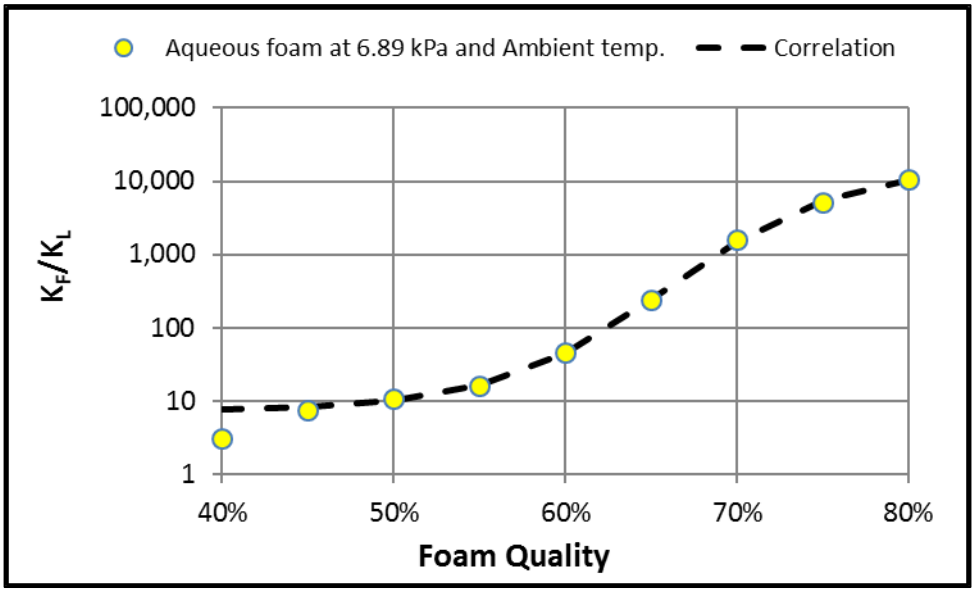

Figure 5.8 K_F/K_L vs. foam quality for aqueous foams at 6.89 MPa (1000 psig) and 23.8 °C (75 °F)

Table 3.3 Dimensionless constants used in Eqn. (5.5)

Parameter	K_F/K_L
a	7.6912
b	0.0508
x_o	0.6596
y_o	2.0135

5.4 Polymer Based Foams

Due to its thermal stability at higher temperature, PAC based foam was used to investigate the effect of temperatures on foam rheology. Tests were conducted at a pressure of 6.89 MPa (1000 psig) and varying temperature and foam quality.

5.4.1 Rheological Analysis

Rheograms of 75% quality foam at different temperatures are shown in Fig. 5.9. It can be depicted from the figures that the wall shear stress generated by the PAC based foam for a given quality and an applied shear rate decreases with temperature, which implies that the apparent viscosity of foam decreases with temperature.

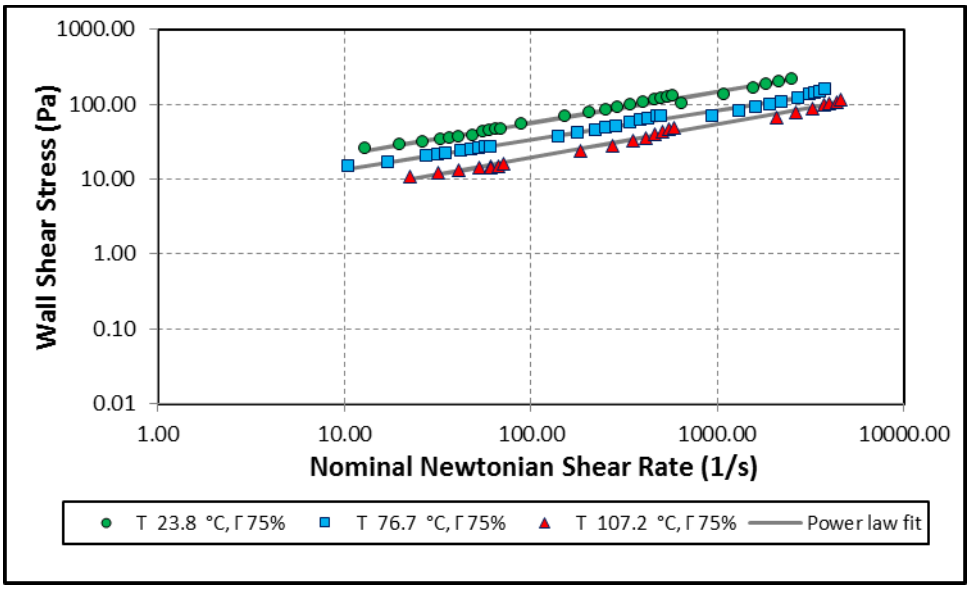

Figure 5.9 Rheogram showing the effect of temperature on PAC based foams at 6.89 MPa (1000 psig)

Rheograms for polymer-based foams obtained at 6.9 MPa and different temperatures are displayed in Figs. 5.10 to 5.12. Some data points are used in the analysis for experiments conduct at high temperature (76.7 and 102.7°C). This is because some of high shear rate experiments were conducted under turbulent flow condition in small and medium pipes. Also, in some cases, measurements from medium and large pipes were below the measuring range of the differential pressure transmitters due to significant reduction in base liquid viscosity at high temperature. The establishment of turbulent flow in the viscometers is verified by determining the Reynolds number and Fanning friction factor and presenting the data in logarithmic

plots. When the actual Fanning friction factor is compared with the theoretical one (f = 16/Re), the onset of turbulence is clearly displayed at Reynolds number of approximately 2400 (Fig. 5.13). The delay on the onset of turbulent is due to fact that power-law fluids have a different critical Reynolds number that dictates the transition to turbulent flow.

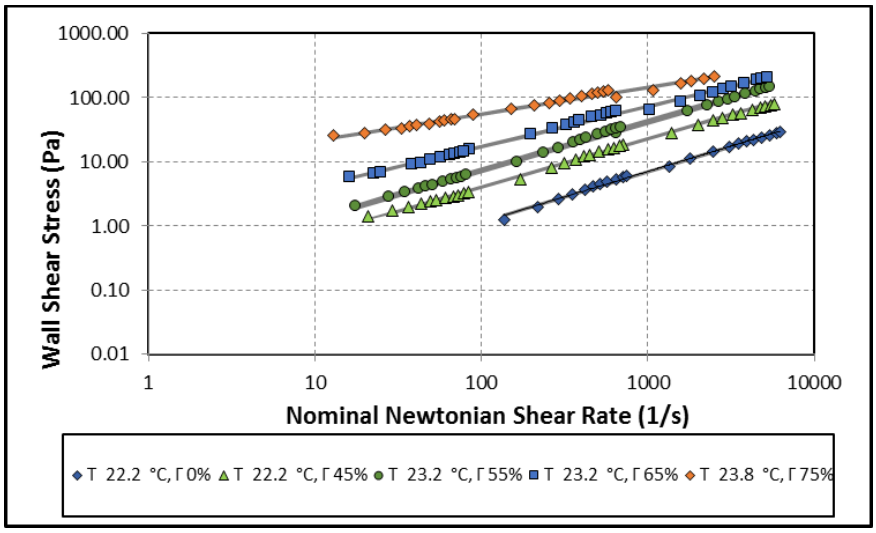

Figure 5.10 Rheogram for PAC based foams at 6.89 MPa (1000 psig) and 23.8 °C (75°F)

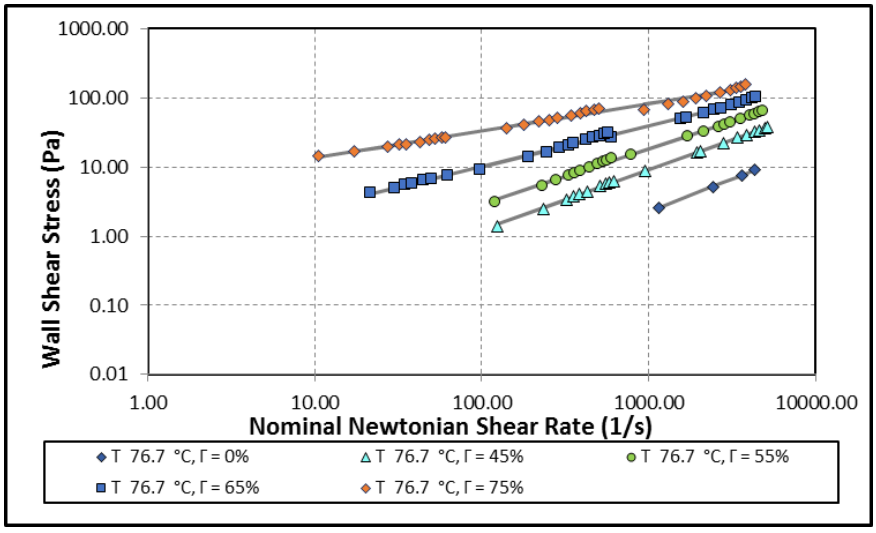

Figure 5.11 Rheogram for PAC based foams at 6.89 MPa (1000 psig) and 76.7 °C (170 °F)

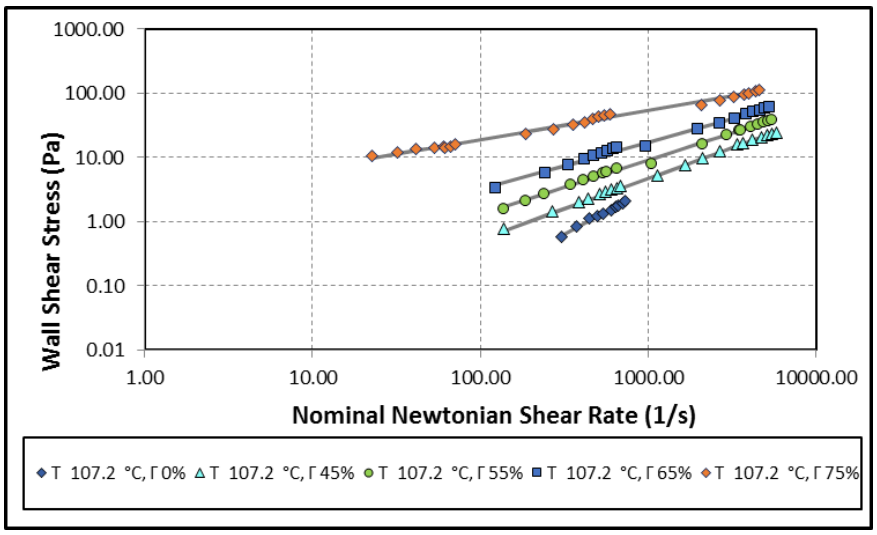

Figure 5.12 Rheogram for PAC based foams at 6.89 MPa (1000 psig) and 102.7 °C (225 °F).

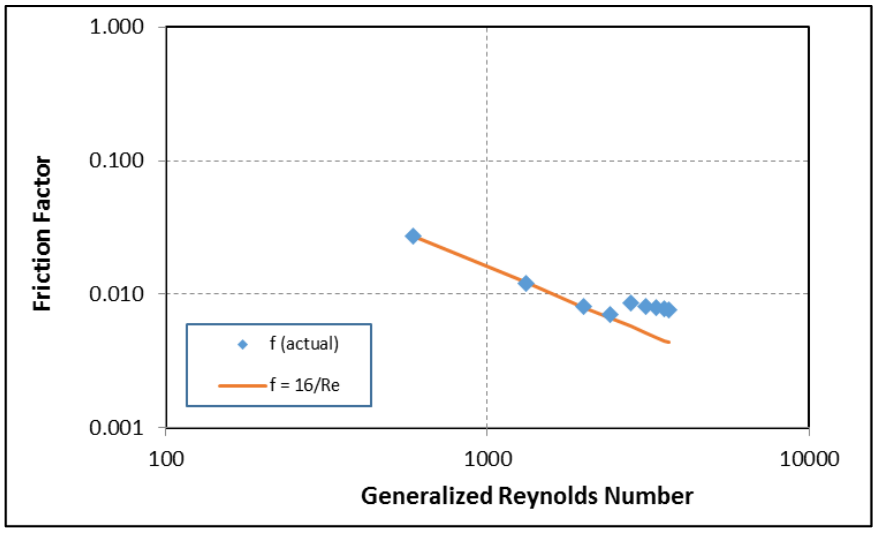

Figure 5.13 Fanning friction factor versus Reynolds number for base liquid at 76.7 °C (170 °F)

5.4.2 Correlation of Power Law Parameters

As mentioned in Section 5.4.2, an observation can be made even in the case of polymer based foams that foam quality is closely related to the rheological properties of foam along with the temperature of the fluid. The correlation developed to relate foam quality to the power law parameters for aqueous foams is adopted for polymer-based

foams. Tables 5.4 to 5.6 present values of $1/n_f$ and K_F/K_L of polymer based foams at different qualities and temperatures.

Table 5.4 Values of $1/n_F$ and K_F/K_L at 23.2°C – PAC foam

Γ	45%	55%	65%	75%
$1/n_F$	1.327	1.331	1.596	2.394
K_F/K_L	4.127	7.613	30.469	248.474

Table 5.5 Values of $1/n_F$ and K_F/K_L at 76.7°C – PAC foam

Γ	45%	55%	65%	75%
$1/n_F$	1.151	1.256	1.683	2.543
K_F/K_L	7.490	24.274	204.804	1642.265

Table 5.6 Values of $1/n_F$ and K_F/K_L at 102.7°C – PAC foam

Γ	45%	55%	65%	75%
$1/n_f$	1.049	1.178	1.354	2.227
K_F/K_L	25.206	97.138	386.928	8345.987

The effect of temperature on flow behavior index is minor although its impact on consistency index ratio is substantial (Figs. 5.14 and 5.15). Flow behavior index of foam is more related to its structure than base liquid properties such as viscosity. Hence, it is more affected by foam quality than other properties of the fluid. Increasing in temperature mainly reduces viscosity of base liquid, as a result, its influence on flow behavior index is limited despite substantial increase in consistency index ratio.

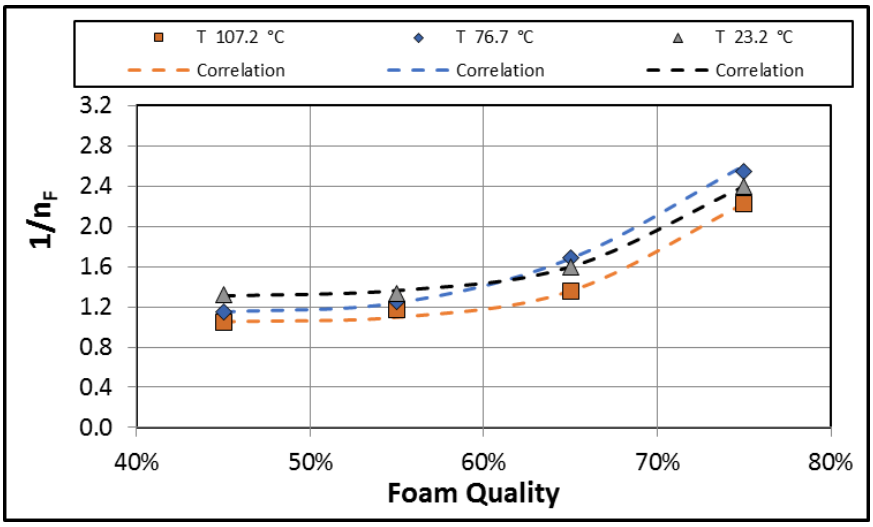

Figure 5.14 $1/n_F$ vs. foam quality for polymer-based foams at 6.89 MPa (1000 psig) and varying temperature.

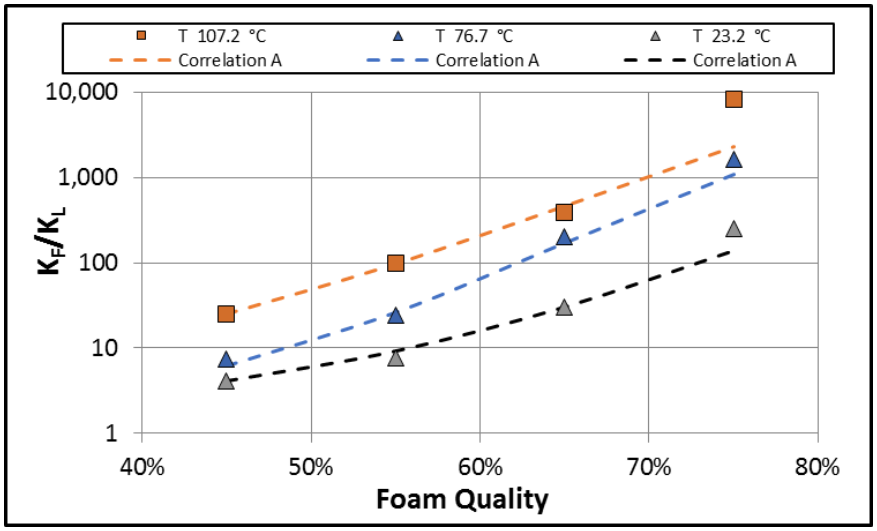

Figure 5.15 K_F/K_L vs. foam quality for polymer-based foams at 6.89 MPa (1000 psig) and varying temperatures with Correlation A.

To develop rheology models for polymer based foams, the parameters presented in Tables 5.7 to 5.9 are correlated with foam quality to the predict flow behavior and consistency index of polymer based foam. Thus:

$$\frac{1}{n_F} = y_0 + \frac{a}{(1+\exp\left(-\frac{(\Gamma - x_0)}{b}\right)} \tag{5.6a}$$

where a, b, y_0 and x_0 are dimensionless parameters, which vary with temperature (Table 5.7).

Table 5.7 Dimensionless correlation parameters of 1/nf vs Γ for polymer-based foams used in Eqn. (5.6a)

T (°C)	**23.2**	**76.7**	**107.2**
	$1/n_F$	**$1/n_F$**	**$1/n_F$**
a	3.6386	2.1314	2.2391
b	0.0639	0.0535	0.0517
x_o	0.8033	0.7066	0.7438
y_o	1.2934	1.1333	1.0410

Similarly, upon extending the earlier correlation developed for aqueous foams in Eqn (5.5) for PAC polymer-based foams, the correlation of consistency index ratio is expressed in similar form as:

$$\frac{K_F}{K_L} = exp\left[y_0 + \frac{a}{(1+\exp\left(-\frac{(\Gamma - x_0)}{b}\right)}\right];\ \Gamma \leq 65\% \tag{5.6b}$$

where a, b, y_o and x_o are dimensionless parameters, which vary with temperature (Table 5.8). Equation (5.6b) is referred to as "Correlation A".

Table 5.8 Dimensionless parameters used in Eqn. (5.6b)

T (°C)	23.2	76.7	107.2
	K_F/K_L	K_F/K_L	K_F/K_L
a	10.688	10.082	12.920
b	0.161	0.129	0.200
x_o	0.790	0.645	0.670
y_o	0.261	0.000	0.000

Figure 5.16 compares predictions of "Correlation A" with measurements. Although results show predominantly good agreement between measurements and predictions, the correlation performs very poor at high quality (75%) and temperature (102.7°C). correlation (Correlation B) is developed for higher quality foams (65 to 75% quality).

$$\frac{K_F}{K_L} = c_1 * e^{\left(\frac{-(\Gamma - c_2)^2}{2{c_3}^2}\right)};\ \Gamma \geq 65\% \tag{5.8}$$

where C_1, C_2 and C_3 are dimensionless parameters, which vary with temperature (Table 5.8). As correlation A applies better for lower qualities and correlation B works better for higher qualities, both were combined and then plotted in Fig 5.16. Correlation A provides good prediction for foam qualities ranging from 45 to 65%.

Table 5.9 dimensionless Correlation parameters used in Eqn. 5.8

T (°C)	23.2	76.7	107.2
c_1	1.447E+12	9.366E+12	1.370E+13
c_2	2.979	2.959	2.188
c_3	0.332	0.329	0.221

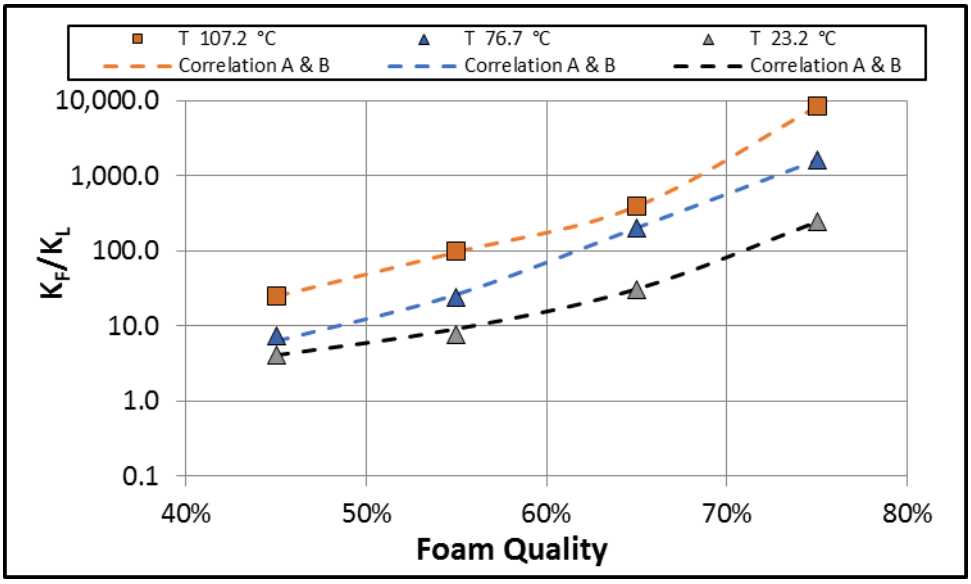

Figure 5.16 K_F/K_L vs. foam quality for polymer-based foams at 6.89 MPa (1000 psig) and varying temperatures with predictions of Correlations A and B

5.5 Yield Stress of Foam

The presence of yield stresses was investigated using the methodology presented in Section 4.2.4, which involves measuring the pressure drop across the test sections and foam generator for static conditions after bringing the foam to a gradual stop after dynamic flow conditions. Results show presence of recoiling phenomenon, which is observed in non-Newtonian fluids. After complete stop of the pump, flow in reverse direction indicated by negative needle valve pressure drop measurement. The pressure drop readings from the viscometers were then converted to wall shear stress using Eqn. (5.1) and then plotted against time along with the pressure drop across the needle valve used in foam generation (Figs. 5.17 to 5.19). A peak or a plateau in the wall shear stress plot is hypothesized as the yield stress at static conditions when supported with the fact that the yielding effect diminishes while the foam degrades with time and the negative pressure differential across the needle valve begins to drop. The wall shear stress

measured at the turning point of the needle valve differential pressure is then plotted on the corresponding rheogram to get a fit of the Herschel-Bulkley model. For both aqueous and polymer-based foams, significant yield stresses were observed only for a foam quality of 75% (Figs. 5.17 to 5.19).

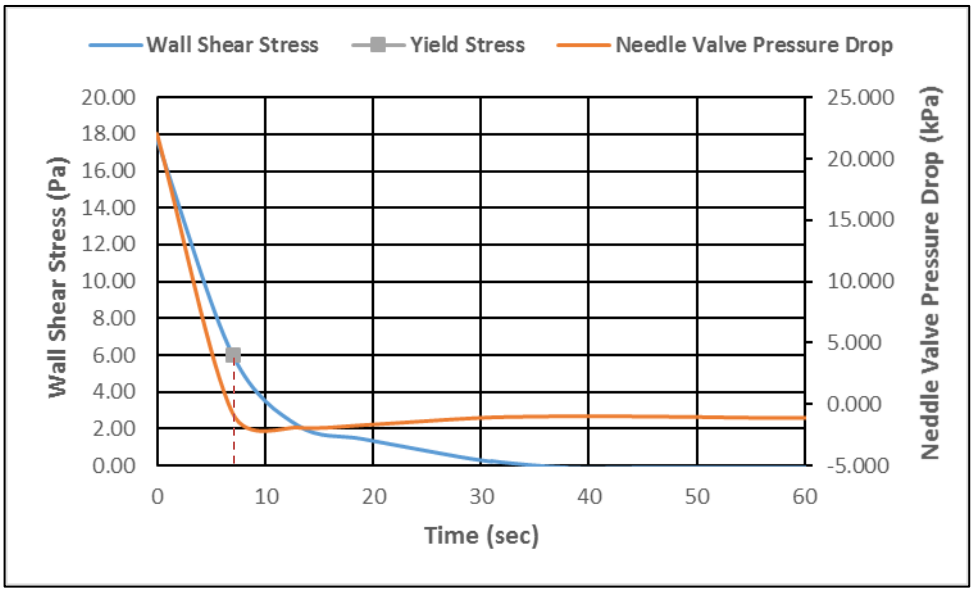

Figure 5.17 Wall shear stress and needle valve pressure drop vs. time for small pipe at static conditions (Aqueous foams Γ=75% 20.68 MPa 23.8°C)

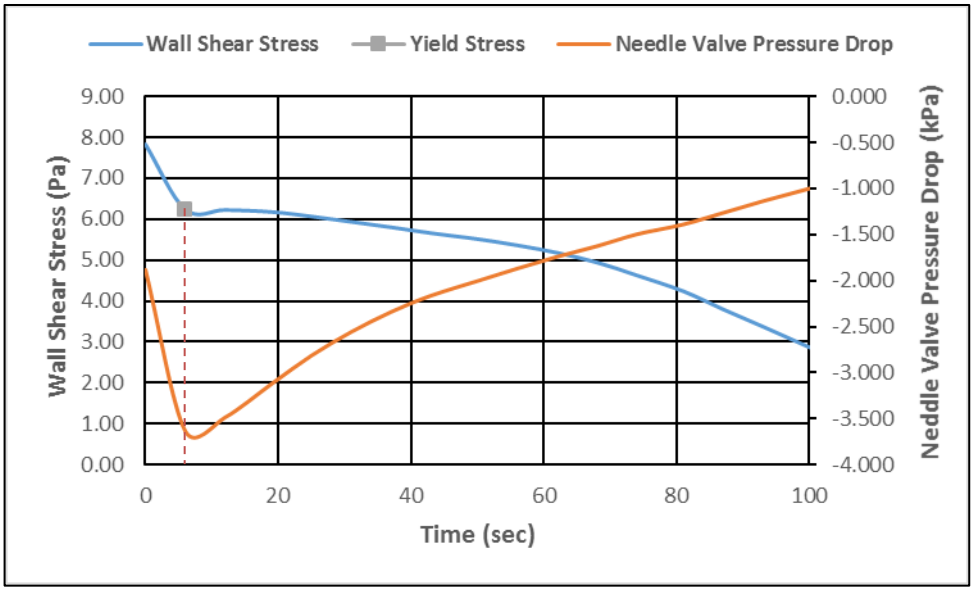

Figure 5.18 Wall shear stress and needle valve pressure drop vs. time for medium pipe at static conditions (Aqueous foams Γ=75% 20.68 MPa 23.8°C)

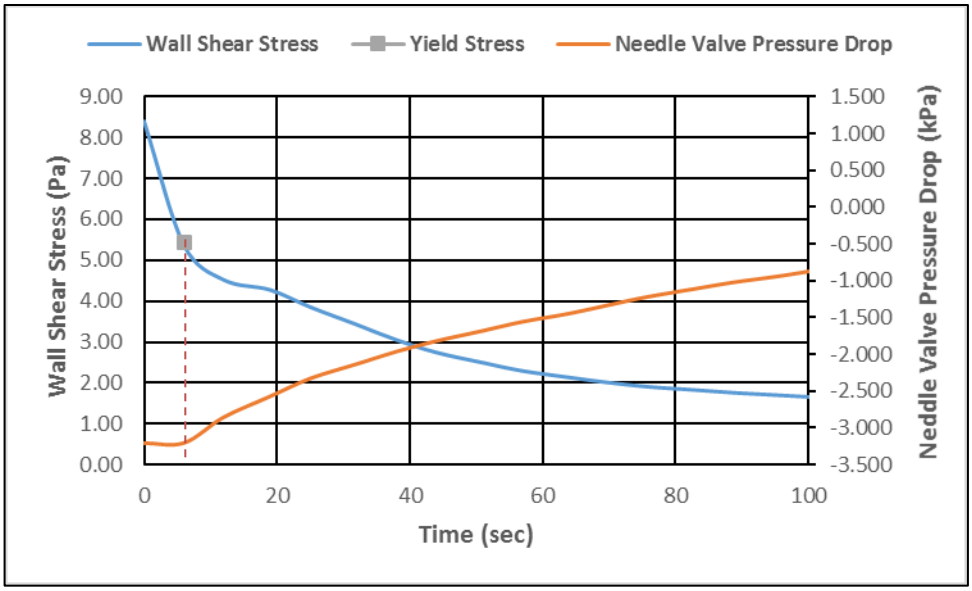

Figure 5.19 Wall shear stress and needle valve pressure drop vs. time for small pipe at static conditions (Polymer-based foams Γ=75%, 6.89 Mpa 23.2°C)

For aqueous foams of 75% quality at 20.68 MPa (3000 psig), 6.0 Pa is chosen as the yield stress value (Fig. 5.18). It was observed in the plateau region of the wall shear stress versus time for medium pipe. For the small pipe, the plateau was observed late. Upon observing the pressure drop across the needle valve, the elastic deformation of the

foam, which induces reverse flow can be envisaged; thus, further reinforcing the yielding behavior of foams. Negative pressure gradient develops due to the fluid's tendency to recoil and the needle valve to some extent preventing reverse flow resulting in entrapment of the fluid. However, with time, the foam degrades and loses its structure and viscosity, then the negative differential pressure is able to induce reverse flow through the needle valve resulting in pressure equalization upstream and downstream of the valve.

For 75% quality, aqueous foam at 20.68 MPa exhibited a yield stress of 6 Pa (Fig. 5.18). Figure 5.20 shows that the Herschel-Bulkley model is a good fit for the above-mentioned yield stress and does not vary to a large extent as compared to the power-law model. The HB model is obtained by plugging the yield stress obtained from Fig. 5.18. Similar result is obtained with polymer-based foam tested at 6.9 MPa and ambient temperature (Fig. 5.21).

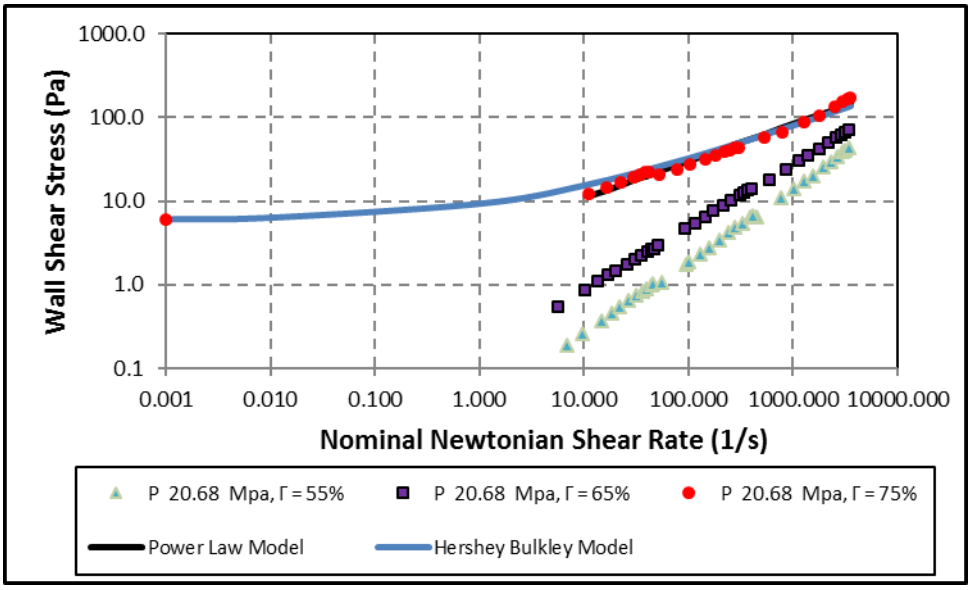

Figure 5.20 Rheogram for aqueous foams with yield stress at 20.68 MPa and 75% quality

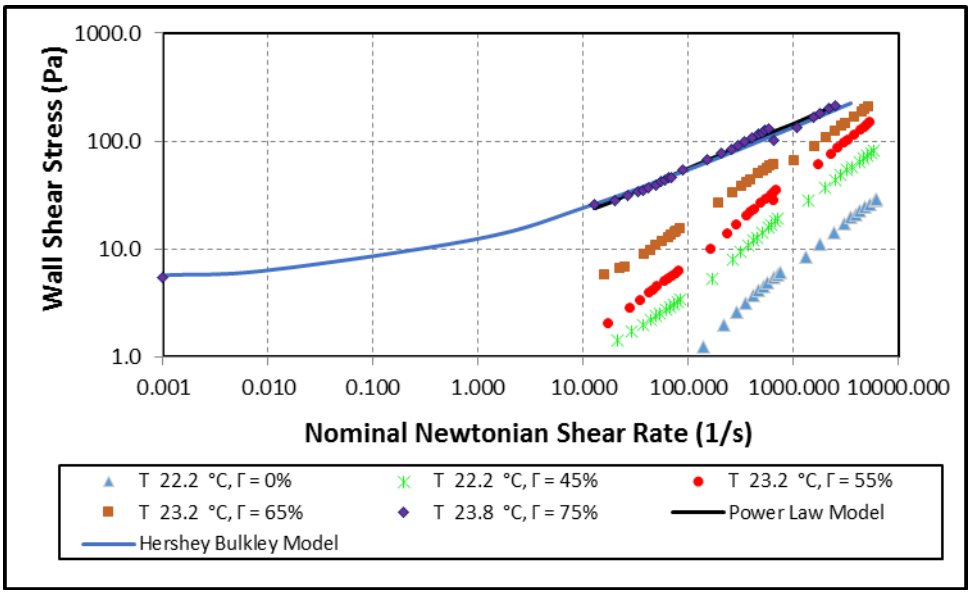

Figure 5.21 Rheogram for polymer-based foams with yield stress at 6.9 MPa and 75% quality

5.6 Comparing Results with Existing Literature

5.6.1 Aqueous Foams

Bonilla and Shah (2000) studied the rheology of aqueous foams at 1000 psi and the results in this study matched their results very closely (Fig. 5.22) at low foam qualities (less than 50%). However, discrepancies exist when foam quality is more than 50%. Viscosity measurements obtained in the current study are higher than the once reported by Bonilla and Shah (2000). The variation could be due to difference in foam generation method (Section 2.3).

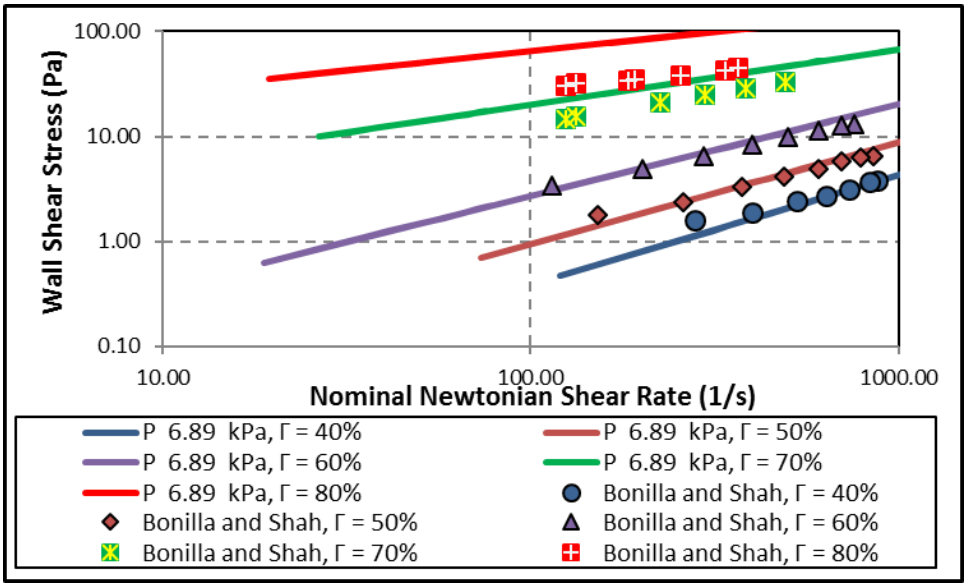

Figure 5.22 Aqueous foam rheology as compared with Bonilla and Shah (2000)

Cawiezel and Niles (1987) studied effect of pressure on nitrogen foam rheology. Their measurements are compared with that of the current study (Fig. 5.23). It is observed that 50% foam qualities had similar results but for qualities of 60% and 70%, there is not a significant difference between the rheograms in their study as when compared to this study. This again can be attributed to the difference in foam generation methods. The viscometer used for the former study is described by Wendorff and Earl (1983), in which, the foam generation section consisted of pumping and vaporizing liquid nitrogen as the source of high-pressure gas. Furthermore, a single pass viscometer was used, and foam quality was controlled using a backpressure regulator. This is attributed to the single pass mode of foam generation creating non-equilibrated foam in viscometers during the measurement. They also conducted foam rheology experiments test pressures of 1000, 3000 and 5000 psig and shear rates ranging from 0 to 2000 s^{-1} and concluded that the apparent viscosity of the foam increases with pressure and the apparent viscosities at a given pressure decreases with increasing shear rate. Their first

inference of the effect of pressure is discussed in Section 2.7. The decrease of apparent viscosity with increasing shear rate is inferred in this experimental study and most other studies (Beyer et al. 1972; Mitchell 1971; Sanghani and Ikoku 1983). However, no particular trend is seen for the apparent viscosity for a given foam quality upon increasing pressures as illustrated in Fig. 5.7

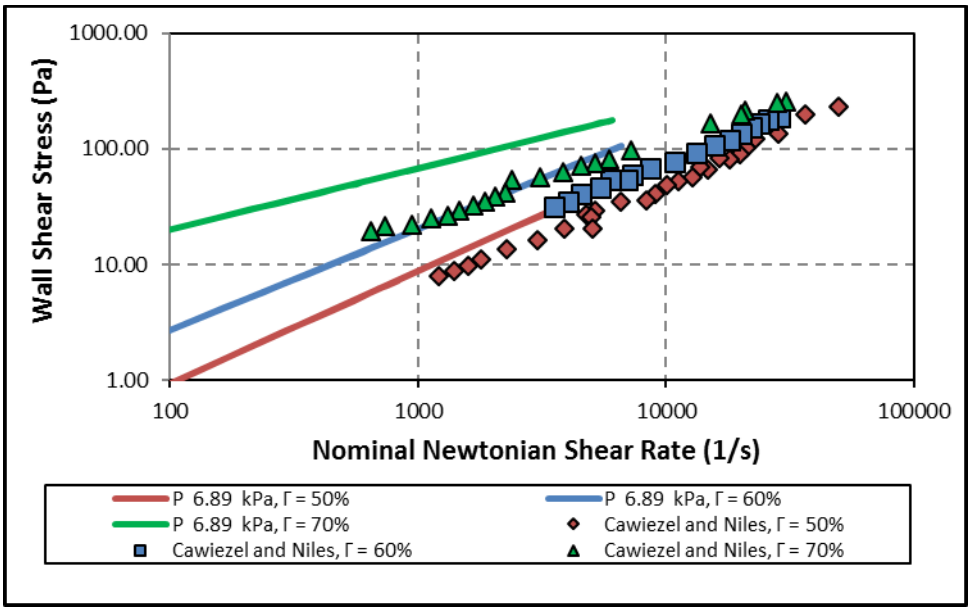

Figure 5.23 Aqueous foam rheology as compared with Cawiezel and Niles (1987)

Harris and Heath (1996) also conducted foam rheology experiments on aqueous foams. They generate their foam with the help of a backpresure regulator (Fig. 5.24). At high qualites, the foam generated in this research has a higher viscosity for nearly the same conditions. This again is primarily due to the structure of the foam that has been developed due to the difference in foam generation methods.

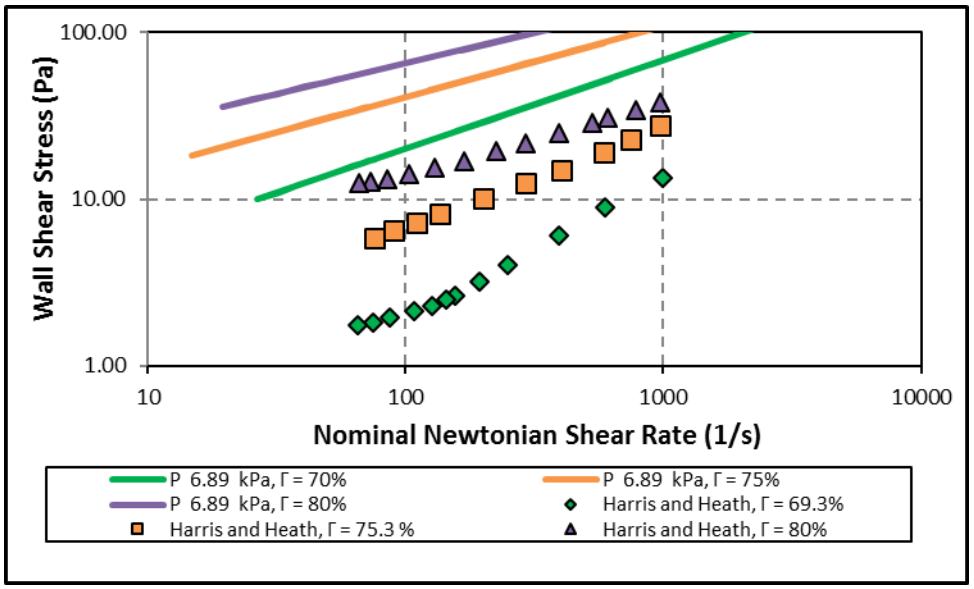

Figure 5.24 Aqueous foam rheology as compared with Harris and Heath (1996)

Comparing the results obtained from this study to similar studies conducted by Mitchell (1971), Sanghani and Ikoku (1983), Beyer et al. (1972), again significant difference is observed. (Fig 5.25) This again is primarily linked to the foam generation method which causes the bubble structure to have distribution such that it generates a higher wall shear stress for a given shear rate.

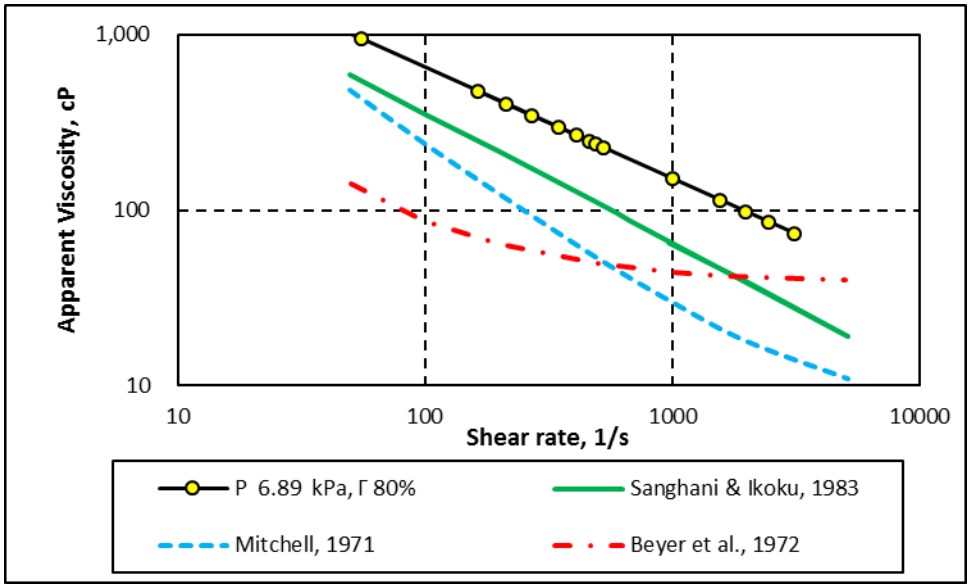

Figure 5.25 Comparing apparent viscosity of 80% quality foam with other works in literature at 6.89 MPa

5.6.2 Polymer-Based Foams

Babatola (2014) used the same foam generation method; nonetheless, when measurements were compared at high qualities, foam that is more viscous was created in this study than what she has reported (Fig. 5.26). The rheogram for 75% in this research is higher than what was seen in Babatola's rheogram of 80%. This can be attributed to the fact, that Babatola's loop set up studied foams at a pressure of 0.69 MPa (100 psi) and also due to the fact that the system volume was nearly 10-fold larger, thus leading to more chances of gravity drainage and bubble coalesence. The former might be the reason the foams were thinner in that loop as compared to what was done in this study.

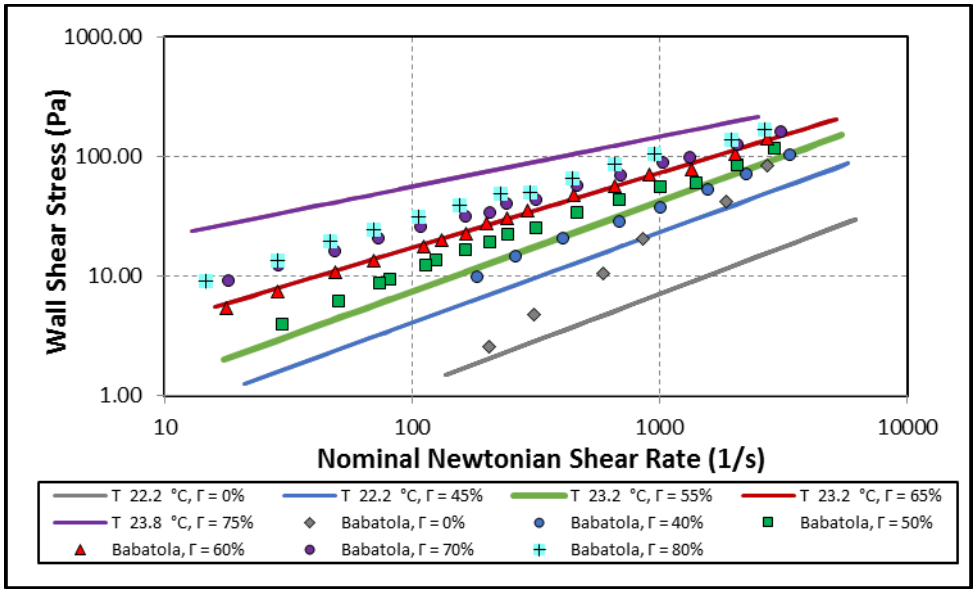

Figure 5.26 Comparing PAC-based foam rheology with work done by Babatola (2014) for the same base liquid (0.25% PAC + Water)

Saintpere et al. (1999) studied three samples of foam in which the first foam tested comprised of 3% PAC and freshwater as the base fluid. The quality used for the rheological study was 90% and a rotational viscometer was used to evaluate foam rheology. Theoretically, a large difference should have been seen between the

rheograms at 75% and 90% due to increasing polyhedral structure of the foams and a higher amount of polymer being used as mentioned in Section 2.6. However, as Fig. 5.27 suggests, this is not the case. Gravity drainage is very likely to happen in a rotational viscometer and might have caused the foams to be thinner while at the time of testing. Also, Saintpere and his team generated foam by agitating the foam solution with 1% surfactant for 2 mins at 2000 rpm. This again is different from the method of foam generation used in this study, which utilizes the pressure drop across a needle valve along with static mixers in a recirculating viscometer to create homogenous and stable foam.

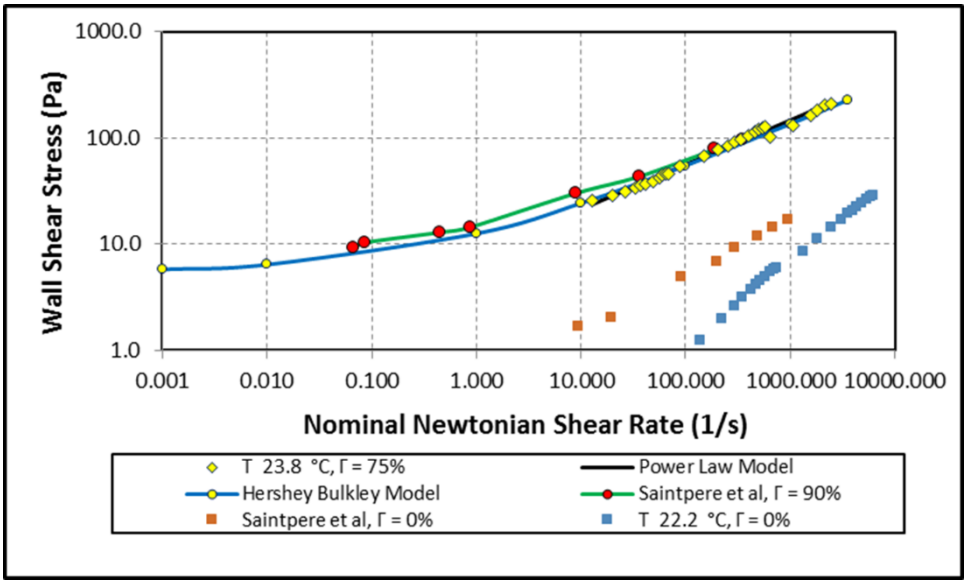

Figure 5.27 Comparing PAC-based foam rheology for 75% quality with work done by Saintpere et al. (1999) for 90% quality

5.6.3 Wall slip effect

As seen from the rheograms in this study, there was no observable wall slip. Since, wall slip wasn't encountered special corrective actions for the measurements was not required as in the case of several other rheological studies (Ahmed et al 2003; Bayer

et al. 1972; Chen et al. 2007; Ozbayoglu et al. 2002; Rojas et al. 2001; and Saintpere et al. 1999) conducted on foams.

5.7 Analyzing Errors in Pressure Drop Measurements

The pressure drop measurements across the tests section was used to calculate the wall shear stress readings for a given shear rate. As illustrated in Fig. 4.5, the foam is tested for a period of 60 secs and while doing so, the pressure drop measurements are continuously recorded. An average of these measurements is selected as the wall shear stress reading when plotted on a rheogram. While utilizing averages, the standard deviation of the data is a key statistic parameter that is used to quantify the amount of variation or error within the data.

The thinnest foam tested, aqueous foam at 40% quality, is used to quantify the variation. Standard deviation felt within the range of 1.5-3.8% of the mean value for pressure drop measurements up to 0.8 kPa and was below 1% for all pressure drop measurements above 0.8 kPa.

Chapter 6: Conclusions and Recommendations

6.1 Conclusions

The following conclusions can be drawn based on the current investigation on rheology of aqueous and polymer-based foams under HPHT conditions using a recirculating pipe viscometer:

- This research shows both conflicting and similar results that have been encountered in the area of foam rheology. This can be primarily attributed to the differences in the foam generation and the methodology in measuring the rheology of foam.
- The no slip boundary condition remains valid for this study as no significant wall slip was observed and hence, no corrections were to be made. This can be attributed to foam generation method, minimal foam expansion in the viscometer and accurate control of test parameters such as temperature, pressure and foam quality.
- The aqueous and polymer-based foams show non-Newtonian behavior and the power-law model was used to describe foam rheology. Empirical correlations are developed with curve fitting techniques, which relate the power-law parameters of aqueous and polymer-based foams to their foam quality.
- Contrary to published studies (Cawiezel and Niles 1987), no significant change in rheological properties was seen for changing pressures at constant foam quality.
- High quality foams (75%) exhibited yield stress under static condition and a preliminary measuring method has been established. More investigation is needed to enhance the new approach. Foams at high temperature did not exhibit measurable yield stress.

6.2 Recommendations

Based on the above conclusions, the following recommendations are given:

- Further studies to be conducted at higher temperatures to study the stability limit of PAC based foams.
- Varying the concentration of PAC to understand its effect on foam rheology at given conditions.
- Additional techniques to better the measurement of yield stresses in foams.
- A viewing section generated sonically or by utilizing other methods, to analyze the bubble size and structure at varying qualities, and quantify their effects on rheology.
- Studying the rheology of higher quality foams (≥ 65%) with quality increment of 2% to account in detail for increasing non-Newtonian behavior.
- Expansion of study to different polymeric base fluids for better understanding of polymer-based foams.

References

Ahmed, R., & Miska, S. 2009. Advanced Wellbore Hydraulics. In B. Aadnoy, I. Cooper, S. Miska, R. Mitchell, & M. L. Payne, *Advanced Drilling and Well Technology.* Society of Petroleum Engineers.

Ahmed, R., Kuru, E., & Saasen, A. 2003. Critical Review of Drilling Foam Rheology. *Annual Transactions of the Nordic Rheology Society, Vol. 11*, 63-72.

Babatola, D. 2014. *Master's Thesis: Rheology of PAC polymer-based foams using pipe viscometers.* University of Oklahoma, Norman.

Ball, P. 2001. *Drilled Wells.* St.Gallen, Switzerland: SKAT, Swiss Centre for Development Cooperation in Technology and Management.

Barnes, H. A., & Walters, K. 1985. The yield stress myth? *Rheologica Acta* , 323-326.

Beyer, A. H., Millhone, R. S., & Foote, R. W. 1972. Flow behavior of Foam as a Well Circulating Fluid. *47th Annual Fall Meeting of the Society of Petroleum Engineers of AIME.* San Antonio, Texas: SPE.

Bird, R. B., Stewart, W. E., & Lightfoot, E. N. 2001. *Transport Phenomena (Second Ed.).* John Wiley & Sons.

Blackwell, B., & Sobolik, K. 1987. *An Experimental Investigation of Pressure Drop of Aqueous Foam in Laminar Tube flow.* Albuquerque, NM: Sandia National Laboratories.

Bonilla, L., & S.N., S. 2000. Experimental Investigation on the Rheology of Foams. *SPE/CERI Gas Technology Symposium.* Calgary, Alberta, Canada.

Brookfield Engineering. 2005. *What is viscosity?* Retrieved from http://www.brookfieldengineering.com/education/what-is-viscosity.asp.

Cawiezel, K. E., & Niles, T. 1987. Rheological Properties of Foam Fracturing Fluids under Downhole Conditions. *SPE Hydrocarbon Economics and Evaluation Symposium.* Dallas, Texas: SPE.

Chen, Z., Ahmed, R., Miska, S., Takach, N., Yu, M., & Pickell, M. 2007. Rheology and Hydraulics of Polymer (HEC) Based Drilling Foams at Ambient. *SPE Journal* 100-107.

Claude, J. F., & John, Q. 1968. *Patent No. US3376924 A.*

Coussot, P. 2014. Yield stress fluid flows: A review of experimental data. *Journal of Non-Newtonian Fluid Mechanics*, 31-49.

Durian, D., & Weitz, D. 1994. Foams. In *Kirk-Othmer Encyclopedia of Chemical Technology, 4th. Edition* (pp. 783-805).

Enzendorfer, C., Harris, R. A., Valko, P., Economides, M. J., Fokker, P. A., & Davies, D. D. 1995. Pipe Viscometry of foams. *Journal of Rheology*, 39 (2), 345-358.

Gas Research Institute. 1997. *Underbalanced Drilling Manual.* Chicago, IL: Gas Research Institute.

Harris, P. 1985. Dynamic Fluid Loss Characteristics of Foam Fracturing Fluids. *Journal of Petroleum Technology* 1847-1852.

Harris, P. 1989. Effects of Texture on Rheology of Foam Fracturing Fluids. *SPE Production Engineering Journal* 249-257.

Harris, P. 1995. A Comparison of Mixed-Gas Foams with N2 and CO2 Foam Fracturing Fluids on a Flow-Loop Viscometer. *SPE Production & Facilities* 197-203.

Harris, P. C., & Heath, S. J. 1998. High-Quality Foam Fracturing Fluids. *SPE Gas Technology Symposium.* Calgary, Alberta, Canada.

Harris, P., & Heath, S. 1996. Rheology of Crosslinked Foams. *SPE Production & Facilities*.

Harris, P., & Pippin, P. 2000. High-Rate Foam Fracturing: Fluid Friction and Perforation Erosion. *SPE Production & Facilities* 27-32.

Harris, P., & Reidenbach, V.1987. High-Temperature Rheological Study of Foam Fracturing Fluids. *Journal of Petroleum Technology*, 613-619.

Heller, J., & Kuntamukkula, M. 1987. Critical Review of the Foam Rheology Literature. *Industrial & Engineering Chemistry Research*, 318-325.

Herzhaft, B. 1999. Rheology of Aqueous Foams: a Literature Review of some Experimental Works. *Oil & Gas Science and Technology*, 587-596.

Holt, R., & McDaniel, J. 2000. Rheology of Foam near the Order-Disorder Phase Transition. *5th Microgravity Fluid Physics and Transport Phenomena Conference*, (pp. 1006-1027). Cleveland, Ohio.

Hutchins, R., & Miller, M.2005. A Circulating Foam Loop for Evaluating Foam at Conditions of Use. *SPE Production & Facilities* 286-294.

Jastrzebski, Z. D. 1967. Entrance Effects and Wall Effects in an Extrusion Rheometer during Flow of Concentrated Suspensions. *Industrail & Engineering Chemistry Fundamentals*, 6 (3), 445-454.

Kenyon, D. 1993. CO2 Foam Slurry Friction Correlations. *SPE Gas Technology Symposium.* Calgary, Alberta, Canada: Society of Petroleum Engineers.

Khade, S., & Shah, S. 2004. New Rheological Correlations for Guar Foam Fluids. *SPE Production & Facilities*, 77-85.

Khalil, C. N., & de Franco, Z. 1989. *Patent No. US4846277 A.*

Khan, S., Schnepper, C., & Armstrong, R. 1988. Foam Rheology: III. Measurement of Shear Flow Properties. *Journal of Rheology*, 69-92.

Kraynik, A. M. *In press.*. Foam flows. *Ann. Rev. Fluid Mech*, 325-357 .

Kraynik, A., Aubert, J., & Rand, P. 1986. Aqueous foams. *Scientific American Magazine* , May 1986, pp. 74-82.

Kroezen, A., Wassink, J., & Bertlein, E. 1988. Foam generation in a rotor—stator mixer: schaumerzeugung in einem rotor—stator mischer. *Chemical Engineering and Processing: Process Intensification* 145-156.

Kroezen, A., Wassink, J., & Schipper, C. 1988. The flow properties of foam. *Journal of Society of Dyers and Colourists*, 393-400.

Li, C., Huang, Y., Sun, X., Gao, R., Zeng, F., Tontiwachwuthikul, P., & Liang, Z. 2017. Rheological properties study of foam fracturing fluid using CO2 and surfactant. *Chemical Engineering Science*.

Lourenço, A., Miska, S., Reed, T., Pickell, M., & Takach, N. 2003. Study of the Effects of Pressure and Temperature on the Rheology of Drilling Foams and Frcitional Pressure Losses. *SPE Annual Technical Conference and Exhibition.* Denver, CO: Society of Petroleum Engineers.

McCabe, W. L., Smith, J. C., & Harriot, P. 1993. *Unit Operations of Chemical Engineering.* McGraw-Hill, Inc.

MI-SWACO. 2007. *Product Sheet: POLYPAC R.* Retrieved from http://www.slb.com/resources/other_resources/product_sheets/miswaco/polypac_r.aspx.

Mitchell, B.1971. Test Data Fill Theory Gap on using Foam as a Drilling Fluid. *Oil and Gas Journal*, 96-100.

Mooney, M. 1931. Explicit Formulas for Slip and Fluidity. *Journal of Rheology 2* 2(2) 210-222.

Ozbayoglu, M., Akin, S., & Eren, T. 2005. Foam Characterization Using Image Processing Techniques. *SPE Western Regional Meeting.* Irvine, CA: Society of Petroleum Engineers.

Ozbayoglu, M., Kuru, E., Miska, S., & Takach, N.2002. A Comparative Study of Hydraulic Models for Foam Drilling. *Journal of Canadian Petroleum Technology, 41*(06).

Patton, J., Holbrook, S., & Hsu, W. 1983. Rheology of Mobility-Control Foams. *Society of Petroleum Engineers Journal*, 456-460.

Phillips, A., Couchman, D., & Wilke, J. 1987. Successful Field Application of High-Temperature Rheology of CO2 Foam Fracturing Fluids. *Low Permeability Reservoirs Symposium.* Denver, CO.

Princen, H. M.1985. Rheology of Foams and Highly Concentrated Emulsions. *Journal of Colloid and Interface Science, Vol. 105, No. 1* 150-171.

Reidenbach, V., Harris, P., Lee, Y., & Lord, D. 1986. Rheological Study of Foam Fracturing Fluids Using Nitrogen and Carbon Dioxide. *SPE Production Engineering*, 31-41.

Rojas, Y., Kakadjian, S., Aponte, A., Márquez, R., & Sánchez, G. 2001. Stability and Rheological Behavior of Aqueous Foams for Underbalanced Drilling. *SPE International Symposium on Oilfield Chemistry.* Houston, TX.

Saintpere, S., Herzhaft, B., Toure, A., & Jollet, S. 1999. Rheological Properties of Aqueous Foams for Underbalanced Drilling. *SPE Annual Technical Conference and Exhibition.* Houston, TX.

Saintpere, S., Marcillat, Y, Bruni, F., & Toure, A. 2000. Hole Cleaning Capabilities of Drilling Foams Compared to Conventional Fluids. *SPE Annual Technical Conference and Exhibition.* Dallas, TX: Society of Petroleum Engineers.

Sanghani, V., & Ikoku, C. U. 1983. Rheology of Foam and its Implications in Drilling and Cleanout Operations. *Energy-Sources Technology Conference and Exhibition.* Houston, TX.

Sani, A.M., Shah, S., & Baldwin, L. 2001. Experimental Investigation of Xanthan Foam Rheology. *SPE Production and Operations Symposium.* Oklahoma City, OK: Society of Petroleum Engineers.

Schlumberger Oilfield Glossary 2017. Rheology http://www.glossary.oilfield.slb.com/Terms/r/rheology.aspx (accessed Mar 2017)

Schramm, L. L. 1994. *Advances in Chemistry; Foams: Fundamentals & Applications in the Petroleum Industry.* Washington D.C.: American Chemical Society.

Sepulveda, J., Falana, O., Kakadjian, S., Morales, J., Zamora, F., DiBiasio, M., . . . S.A, T. 2008. *Oil-Based Foam and Proper Underbalanced-Drilling Practices*

Improve Drilling Efficiency in a Deep Gulf Coast Well. Denver, CO: Society of Petroleum Engineers.

Sherif, T., Ahmed, R., Shah, S., & Amani, M. 2015. Rheological and wall-slip behaviors of polymer based drilling foams. *ASME 2015 34th Internation Conference on Ocean, Offshore and Arctic Engineering.* St John's, Newfoundland, Canada.

Sherif, T., Ahmed, R., Shah, S., & Amani, M. 2015. Rheological behavior of oil-based drilling foams. *Journal of Natural Gas Science and Engineering 26*(Sept 2015), 873 - 882.

Tan, H., & McGowen, J. 1991. Friction Pressure Correlation for CO2 Foam Fluids. *Low Permeability Reservoirs Symposium.* Denver, CO: Society of Petroleum Engineers.

Thondavadi, N., & Lemlich, R. 1985. Flow properties of foam with and without solid particles. *Industrial & Engineering Chemistry Process Design and Development*, 748-753.

Tilton, J. N. 2008. Perry's Chemical Engineers' Handbook. In J. N. Tilton, *Perry's Chemical Engineers' Handbook* (pp. 6.4 - 6.5). The McGraw-Hill Companies.

Viking Drilling. 2017. *Underbalanced Equipment and Services*. (2017 version) http://www.viking-drilling.com/underbalanced-equipment-and-services (accessed Feb 2017)

Wendorff, C. L., & Earl, R. B. 1983. Foam Facturing Laboratory. *58th Annual Technical Conference and Exhibition.* San Francisco, CA: Society of Petroleum.

Nomenclature

Γ – Foam quality (%, fraction)

Ca – Capillary number

σ - Interfacial tension or surface tension (N/m^2)

γ - Shear rate (s^{-1})

η_f - Foam viscosity (cP)

τ - Shear stress (Pa)

τ_y - Yield stress (Pa)

μ_o - Plastic Bingham viscosity (cP)

μ_a/μ_e – Apparent viscosity (cP)

U_{slip} – Slip velocity (m/s)

β – Slip coefficient (m/Pa.s)

τ_w – Wall shear stress (Pa)

β_c – Modified slip coefficient (m^2/Pa.s)

n - Flow behavior index/power-law index, (-)

K - Consistency index ($Pa.s^n$)

Re - Reynolds number (-)

P – Pressure (Pa)

U – Average velocity (m/s)

ρ_{foam} – Density of foam (kg/m^3)

ρ_{gas} – Density of gas (kg/m^3)

ρ_{gas} – Density of liquid (kg/m^3)

K_F – Foam consistency index ($Pa.s^n$)

K_F – Liquid consistency index ($Pa.s^n$)

n_F – Foam flow behavior index (-)

Appendix A: Tables for power-law & Herschel-Bulkley parameters

Table A.1 Power-law parameters for aqueous foams at 6.89 MPa (1000 psig) and 23.8°C(75 °F)

Γ	n (-)	K_f (Pa.s^n)	R^2
40%	1.05	0.003	1
45%	0.98	0.007	1
50%	0.97	0.011	1
55%	0.96	0.017	0.999
60%	0.88	0.047	0.999
65%	0.72	0.237	0.998
70%	0.53	1.57	0.995
75%	0.42	5.172	0.994
80%	0.37	10.59	0.988

Table A.2 Power-law parameters for aqueous foams at 13.78 MPa (2000 psig) and 23.2 °C (75°F)

Γ	55%	65%	75%
n (-)	0.88	0.73	0.40
K_f (Pa.s^n)	0.032	0.204	5.592
R^2	0.998	0.997	0.987

Table A.3 Power-law parameters for aqueous foams at 20.68 MPa (3000 psig) and 23.2 °C (75°F)

Γ	55%	65%	75%
n (-)	0.87	0.75	0.44
K_f (Pa.s^n)	0.035	0.144	3.446
R^2	0.999	1.000	0.983

Table A.4 Rheogram for PAC based foams at 6.89 MPa (1000 psig) and 23.8 °C (75°F)

Γ	45%	55%	65%	75%
n (-)	0.75	0.75	0.63	0.42
K_f (Pa.s^n)	0.120	0.220	0.882	7.196
R^2	0.999	0.997	0.997	0.990

Table A.5 Rheogram for PAC based foams at 6.89 MPa (1000 psig) and 76.7 °C (170°F)

Γ	45%	55%	65%	75%
n (-)	0.87	0.80	0.59	0.39
K_f (Pa.s^n)	0.022	0.071	0.598	4.795
R^2	0.999	0.998	0.998	0.992

Table A.6 Power-law paramters for PAC based foams at 6.89 MPa (1000 psig) and 102.7 °C (225 °F).

Γ	45%	55%	65%	75%
n (-)	0.95	0.85	0.74	0.45
K_f (Pa.s^n)	0.006	0.025	0.100	2.147
R^2	1.000	0.999	0.994	0.993

Table A.7 Herschel-Bulkley parameters for PAC based foams at 13.78 MPa (2000 psig) and 23.2 °C (75°F)

Γ	75%	τ_w (Pa)	8U/D (s^{-1})
		0.001	7.25
n (-)	0.40	0.01	7.78
		1	12.49
K_f (Pa.s^n)	5.592	10	21.00
		100	42.45
τ_y (Pa)	6.90	1000	96.53
		3660	157.83

Table A.8 Herschel-Bulkley parameters for PAC based foams at 20.68 MPa (3000 psig) and 23.2 °C (75°F)

Γ	75%	**τ_w (Pa)**	**8U/D (s^{-1})**
		0.001	6.16
n (-)	0.44	0.01	6.45
		1	9.45
K_f (Pa.s^n)	3.446	10	15.58
		100	32.63
τ_y (Pa)	6.00	1000	80.01
		3572	136.25

Table A.9 Herschel-Bulkley parameters for PAC based foams at 20.68 MPa (3000 psig) and 23.2 °C (75°F)

Γ	75%	**τ_w (Pa)**	**8U/D (s^{-1})**
		0.001	5.80
n (-)	0.42	0.01	6.45
		1	12.60
K_f (Pa.s^n)	7.196	10	24.23
		100	54.66
τ_y (Pa)	5.40	1000	134.26
		3572	224.71